

**ENCAPSULATION OF PARTICLES IN CROSSLINKED HYDROGEL NETWORKS:
PARTICLES DISTRIBUTION OPTIMIZATION**

by

Karem Alessandra Court Pinto

A thesis submitted in partial fulfillment of the requirements for the degree of

MASTER OF SCIENCE
in
CHEMICAL ENGINEERING

UNIVERSITY OF PUERTO RICO
MAYAGÜEZ CAMPUS
2010

Approved by:

Patricia Ortiz Bermúdez, PhD
Member, Graduate Committee

Date

Juan López Garriga, PhD
Member, Graduate Committee

Date

Aldo Acevedo Rullán, PhD
Member, Graduate Committee

Date

Madeline Torres Lugo, PhD
President, Graduate Committee

Date

Rodolfo Romañach Suarez, PhD
Representative of Graduate Studies

Date

David Suleiman Rosado, PhD
Chairperson of the Department

Date

ABSTRACT

Particle encapsulation in polymer systems has been used in several industrial applications in the biomedical and pharmaceutical fields. The main challenge in particle encapsulation is to obtain a homogeneous particle distribution through the membrane. For the pharmaceutical industry this is a key issue as it is imperative to know how active ingredients in the form of particles are distributed within a therapeutic dose. Current literature lacks information regarding the understanding of the physicochemical interactions of particles distributed in polymeric membranes. Thus, this investigation focuses on the examination of the physicochemical interaction between particles and crosslinked hydrogels networks for the creation of homogeneous dispersed membranes. To achieve this objective the effects of particle charge, concentration and size will be examined to ascertain their effect on particle's dispersion within the matrix. Finally, the effects on the network mechanical properties and rheology will be investigated.

RESUMEN

La encapsulación de partículas en polímeros es ampliamente utilizada en biomedicina y en la industria farmacéutica. El reto principal que presenta la industria farmacéutica es obtener membranas con partículas homogéneamente distribuidas. Actualmente la industria farmacéutica está interesada en conocer como se distribuyen las partículas de los ingredientes activos en geles y membranas poliméricas. La literatura científica realizada hasta el momento no reporta un estudio que explique las causas fisicoquímicas que afectan la distribución de partículas en membranas poliméricas. Por tal razón esta investigación consiste en determinar las propiedades fisicoquímicas que afectan la interacción entre partículas e hidrogeles entrecruzados para crear membranas homogéneamente distribuidas. La carga de la partícula, concentración y tamaño y la carga de la membrana serán examinadas como posibles factores que afectan la distribución de partículas en membranas poliméricas. Además, las propiedades mecánicas y reológicas de los hidrogeles serán analizadas.

To my dearest family

ACKNOWLEDGEMENTS

First at all, I thank God for give me the strength and will to live everyday, also to start any new initiative.

I want to stand that this investigation would not be possible without the support of different persons and institutions. With their contributions it was possible to conclude this research.

Special gratitude should I pay to my dearest family. They have been extremely supportive throughout this stage of my life. They have encouraged me not to give up, but to fight for what I want instead. They have taught me that in life, challenges are hard but the sense of success you gain from them is well worth all the effort.

For that and more, I cherish them with all my heart and dedicate this achievement to them. In the academic, my sincere tribute to the University of Puerto Rico and Chemical Engineering Department, they gave me the opportunity of continue my academic studies and for gave me the necessary knowledge and implements to finish this research.

Additionally, it is important to recognize the support of different persons. The faculty, to the professor Madeline Torres for gave me the opportunity to work with her and in this new project. It would have not being possible to achieve the knowledge and final objectives without her guidance. Special thank you to Professor Rodolfo Romanach who help me to understand the chemistry of the investigation and professor Aldo Acevedo who help with the last objective. Professor Carlos Velazquez and ERC-SOPS for the financial support.

I would like to thank to other important people who help in this investigation, Janet Mendez who was the first to teach to work in the laboratory and for hers continuous advice. Jackeline Jerez and Vivian Florian thank for all the time and patience.

Finally, but not last, my friends who play an important role in my life. To Hector Luis and Celimar who help me a lot when I was new at the laboratory. Mario y Liliana for always be there for me. Sonia, Sully and their family that now are my family.

TABLE OF CONTENT

ABSTRACT	II
RESUMEN	III
TABLE OF CONTENT	vi
1.1 Motivation	1
1.2 References	3
2 BACKGROUND	4
2.1 Particle Encapsulation	4
2.2 Hydrogel membrane	5
2.3 REFERENCES	8
3 LITERATURE REVIEW	10
3.1 REFERENCES	14
4 OBJECTIVES	15
5 FACTORIAL DESIGN	16
5.1 REFERENCES	20
6 Qualitative and Quantitative Determination of Particle Distribution Within Hydrogels Membranes.	21
6.1 Background	21
6.2 Spatial Sample distribution with Near Infrared Chemical	23
6.3 Materials and methods	25
6.4 Results	28
6.4.1 Zeta Potential	28
6.4.2 Near Infrared Chemical Imaging	33
6.5 Conclusions on particles distribution	67
6.6 References	68

7 Effect of Encapsulated Particles on the Mechanical Properties of Crosslinked Hydrogels...... 70

7.1 Introduction.....70

7.2 Literature Review71

7.3 Materials and Methods74

7.4 Results75

7.5 Conclusion and recommendations 79

8 Conclusions 81

LIST OF FIGURES

Figure 6.1	Near Infrared Chemical Imaging hypercube	22
Figure 6.2	Chemical molecules of monomers and crosslinker of the hydrogels	31
Figure 6.3	Functional groups of silica from Corpuscular	31
Figure 6.4	Zeta Potential for functionalized silica particles at various pH's.	32
Figure 6.5	Spectra for a) DMAEM b) HEMA, c) MAA to show NIR penetration	34
Figure 6.6	a) DMAEM NIR spectra with and without particles, b) HEMA NIR spectra with and without particles, c) MAA NIR spectra with and without particle.	36
Figure 6.7	DMAEM with negative 100 μm particles, a) Conventional microscopy image, b) NIR chemical imaging at 1390 nm , c) NIR chemical imaging 2260 nm.	38
Figure 6.8	NIR chemical imaging for carbon –hydrogen bong at 1730nm. Conventional microscopy and NIR chemical imaging	40
Figure 6.9	NIR chemical imaging water band 1920 nm for encapsulated and non-encapsulated particles	41
Figure 6.10	NIR Chemical image and SEM for membrane positive with 100 μm silica particles and low concentration with different charges	45
Figure 6.11	NIR Chemical image and SEM membrane positive with 100 μm silica particles and high concentration with different charges	46
Figure 6.12	NIR Chemical at 1390 nm and SEM membrane neutral with 100 μm silica particles and low concentration with different charges.	47
Figure 6.13	NIR Chemical image and SEM images for neutral membrane with 100 μm silica particles and high concentration (4.4 w/w%) with different charges	48
Figure 6.14	NIR chemical image and SEM images for negative membrane with 100 μm silica particles with low (2.2 w/w%) concentration composed of different charges.	49
Figure 6.15.	NIR Chemical image and SEM for negative membrane with 100 μm silica particles and high concentration (4.4 w/w%) with different charges	50
Figure 6.16	Example of a binary image of DMAEM with silica negative charge particles at 2260 nm. A) Conventional image, b) Chemical imaging, c) Binary image.	52
Figure 6.17	Example of a binary image of DMAEM with silica negative charge	52

	particles at 2260 nm with 16 equal squares.	
Figure 6.18	Average R particle distributions in positive hydrogels with 100 μm , different particle charge and two particle concentration.	54
Figure 6.19	Average R particle distributions in negative hydrogels with 100 μm , different particle charge and two particle concentrations	54
Figure 6.20	Average R particle distributions in neutral hydrogels with 100 μm , different particle charge and two particle concentrations	56
Figure 6.21	Positive membrane with 1 μm particles and low (2.2 w/w%) and high (4.4 w/w%) concentration SEM and NIR images at 2260 nm...	62
Figure 6.22	Negative membrane with 1 μm particles and low (2.2 w/w%) and high (4.4 w/w%) concentration SEM and NIR images at 2260 nm...	63
Figure 6.23	Neutral membrane with 1 μm particles and low (2.2 w/w%) and high (4.4 w/w%) concentration SEM and NIR images at 2260 nm...	64
Figure 6.24	Average R particle distributions in positive hydrogels with 1 μm , different particle charge and two particle concentrations	65
Figure 6.25	Average R particle distributions in neutral hydrogels with 1 μm , different particle charge and two particle concentrations.	65
Figure 6. 26	Average R particle distributions in negative hydrogels with 1 μm , different particle charge and two particle concentration	66
Figure 7.1	Storage modulus in function of time of HEMA hydrogel with 100 μm 4.4 w/w% negative particles	76

LIST OF TABLES

Table 5.1.	Four Factors of the design	18
Table 5.2.	Factorial Design	18
Table 6.1	Hydrogel composition.	27
Table 6.2	Monomer solution pH and pKa	30
Table 6.3	pI silica particles	30
Table 6.4	Rejected percent of the null hypothesis for low and high particles concentration.	58
Table 6.5	Rejected percent of the null hypothesis for low and high particles concentration.	60
Table 7.1	Storage modulus for different charge hydrogel with encapsulated silica particles of 100 μm	78
Table 7.2	Storage modulus for different charge particles in different charge hydrogel of 100 μm	78
Table 7.3	Storage modulus for different silica particles with negative charge concentration in DMAEM (positive) hydrogel of 100 μm	78

LIST OF APPENDIX

Appendix I.	NIR Chemical image of HEMA and MAA	83
Appendix II.	Calculus model for hypothesis test in quantitative analysis	84
Appendix III.	NIR Chemical Images of 100 nm particles encapsulation	85

1 INTRODUCTION

1.1 Motivation

Particle encapsulation is used in several industries including agricultural, pharmaceutical, cosmetic, ink, and paint. Also, such systems are important in fields such as adhesive, textile, optics, and electronics. Recently, a new technology called film strips have been employed for the delivery of therapeutic agents [1]. Film strips are fast dissolving films for oral delivery of active and inactive ingredients such as supplements, vitamins, and pharmaceuticals for human or animals. Films strips can be made of different sizes, shapes and properties. They deliver the intended dose with accuracy via the oral route. This route is the most desirable because is painless, and the dosage can be easily adjusted [1, 2]. Such systems possess the challenge that the particulate that includes the active ingredient must be homogeneously dispersed within the membrane to guarantee equal dosing.

Recent studies have examined the encapsulation of particles in different systems such as liposomes, miniemulsions, emulsions, and polymeric networks such as hydrogels. The later are defined as hydrophilic networks which are created by the reaction of linear polymeric precursors with a crosslinker. They differ from physical hydrogels because chemical hydrogels form covalent attachment between two chains. These links provide physical stability when exposed to temperature and different solvents whereas physical hydrogels present weak intermolecular association, reversible bonds or groups, generated by Van der Waals forces, electrostatic attractions or hydrogen bonding [3].

Hydrogels had been used in the biomedical field for drug delivery, contact lenses, catheters, biosensors and wound dressing because they have special properties as they can retain large amount of water and are insoluble since they have physical or chemical crosslink in its structure [4]. Crosslinked hydrogels also have physical properties similar to that of living tissue [5]. These properties make them excellent systems to model and study the chemistry of particle encapsulation since these membranes are not affected by external factors such as temperature or a dissolvent.

This investigation focuses on the special properties of hydrogels and the need to study the interaction of these particles with the encapsulation shell. The understanding on how the size, charge and composition affect the homogeneous distribution of particles within a matrix is of utmost importance. In addition the mechanical properties and rheology of the membranes will be studied for particle encapsulation. Silica-based particles with various chemical moieties will be employed. Such understanding should serve as a model for different systems of particle encapsulation.

1.2 References

[1] S. Jodi and J. Jodiel, "Vitasolve Dissolving Film Strips with Supplements Pharmaceutical Drug(rx), + Vitamins", United State Patent Application Publication, US 2005/0088632 A1, 2005.

[2] C. Wischke¹, S. P. Schwendeman, "Principles of encapsulating hydrophobic drugs in PLA/PLGA microparticles", *International Journal of Pharmaceutics*, vol. 364, pp. 298–327, 2008.

[3] R. Larson, *The Structure and Rheology of Complex Fluids* Oxford University Press, 1999

[4] C. Bell and N. Peppas, Water, solute and protein diffusion in physiologically responsive hydrogels of poly(methacryli6 acid-g-ethylene glycol), *Biomaterials*, pp.1203-1218, 1996.

2 BACKGROUND

Particle encapsulation within membranes can produce homogenous or heterogeneous particle distribution. This distribution depends on several factors and it is important to know which methods have been used to encapsulate particles.

2.1 Particle Encapsulation

Particles encapsulated in polymers have become more popular because they offer interesting and multiple applications. Such systems are used in the encapsulation of pigments for the manufacture of cosmetics, inks and paints. They are also important in agricultural and pharmaceutical industries to attain the controlled-release of pesticides and drugs. The encapsulation of inorganic particles in polymers has also other applications in fields such as adhesive, textile, optics and electronics [1].

An appropriate encapsulation system should permit the adjustment of membrane shell side, pore size, mechanical strength, and surface potential. It should also give enough stability to accomplish delivery. The most common encapsulation systems are liposomes, miniemulsions and hydrogels. [2]

The first method to be discussed is that of liposomes, which are self-assembled vesicles consisting of a spherical bilayer structure surrounding an aqueous core domain. They are biocompatible and are easy to prepare. Liposomes on the nanoscale have shown to be excellent for the delivery of nucleic acids, proteins, and chemotherapeutic agents such as doxorubicin [3]. Current investigations have not been capable to create a liposome that resist drugs leakage during the transportation to the target and be able to release their content fast in the specific target area. Strategies to improve the control of the drug release consists in incorporating components to reach thermal, pH, photochemical, or enzymatically activated release, but these systems always have agents that encourage release in circulation and in the site of interest [5].

Another system is miniemulsion polymerization that consists of a heterophase arrangement in which stable nanodroplets are dispersed in a continuous phase. Miniemulsion is more stable than usual emulsions and can be employed for the

preparation of latex suspensions with particle sizes among 50 to 500 nm with uniform particle distribution [4]. For example, poly(methyl methacrylate) has been used to encapsulate titanium dioxide particles[1] for the remediation of wastewater streams by photocatalysis [6]. Emulsion and miniemulsion polymerizations are also used in the water-based paint and ink formulations industry where one of the most challenging tasks is to disperse pigments, maintain the quality of that dispersion throughout manufacturing and/or storage, and through the film formation process to the final coating. This encapsulation method in the pigment industry has weaknesses such as low efficiency and the particles need several complex treatments before the encapsulation. Most methods need low concentration of particles, thus pigments loose stability and form aggregates. [7]

Finally, hydrogel membranes are hydrophilic polymer networks that can retain large amounts of water or biological fluids [8]. They have been used for targeted drug delivery in the body, because they are biocompatible, can be biodegradable and easily dispersed in water. Microscale hydrogels have been used for cell encapsulation, cell-based therapy, and bioprocess applications [9]. The advantage of hydrogels is that the swelling of the membrane can be controlled by changing the temperature and pH of its environment. When the hydrogel swells-up the drug or biological substance is liberated [10,11]. Most of the reported hydrogels are not biodegradable, which is a problem for its to use as drug delivery systems [12].

The main challenge in particle encapsulation is the particle distribution through the membrane. This distribution can be homogenous or heterogeneous. In industry encapsulation of particles is broadly used. To create a better product it is important to understand the interaction between the particles and the medium where they are encapsulated and how this interaction affects their distribution.

2.2 Hydrogel membrane

Hydrogels have been used for encapsulation of organic materials like cells and proteins and some are considered intelligent carriers for drug delivery. They have a

great potential in the biomedical field [8,9,10]. These membranes can be designed with specific characteristics like its charge, composition, mesh size, amongst others and resist changes in temperature and different solvents that made them excellent candidates for particle encapsulation

Hydrogel membranes are hydrophilic polymer networks that can retain large amounts of water or biological fluids [8]. The dissolution of the polymer in water is not allowed due to chemical crosslinks of the hydrophilic polymer chains. The crosslinking can be chemical or physical. [13]

Their most important feature is their physical properties similar to soft living tissue like the high water content, soft and rubbery consistency that reduces the irritation to adjacent tissue, low interfacial tension and low tendency for proteins and cells to adhere to the surface of the hydrogel [4,5]. Hydrogels can be classified based on characteristics such as: the nature of side groups, neutral or ionic; mechanical and structural performance, affine or phantom; method of preparation, homo- or co-polymer, physical structure; amorphous, semicrystalline, hydrogen-bonded, supermolecular, hydrocolloidal or responsiveness to physiologic environment stimuli, pH, ionic strength, temperature, electromagnetic radiation, amongst others. [14]

Hydrogels have been widely used in the biomedical and pharmaceutical field. Several studies have been performed to improve their physical and chemical properties at the molecular level for controlled drug delivery. The quick response of these structures allows for drug release that depends on the conditions of the environment. For example, hydrogels based on PEG and methacrylic acid has been employed in the oral delivery of insulin and calcitonin [15]. The main goal of controlled drug delivery systems consists of providing the drug of interest at a specific predetermined release rate to accomplish the specific therapeutic needs. Hydrogels have special properties which make them highly considered as one of the ideal future controlled release system. [16]

Crosslinked hydrogels are excellent membranes models because they are chemically crosslinked. These chemical bonds make them stable in temperature

changes or solvent environments. Other important advantage of these hydrophilic gels is that the charge of the membrane can be set according to the monomer used and are easy to make.

2.3 REFERENCES

- [1] E. Bourgea-Lami and J. Lang, "Encapsulation of Inorganic Particles by Dispersion Polymerization in Polar Media" *Journal of Colloid and Interface Science*, vol. 197, 293-308, 1998.
- [2] X. Shi, S. Wang, X. Chen, S. Meshinchi, and J. R. Baker, "Encapsulation of Submicrometer-Sized 2-Methoxyestradiol Crystals into Polymer Multilayer Capsules for Biological Applications", *Molecular Pharmaceutical*, vol. 2, pp. 144-151, 2006.
- [3] S. Lee, H. Chen, C. M. Dettmer, T. V. O'Halloran, and S. T. Nguyen, "Polymer-Caged Liposomes: A pH-Responsive Delivery System with High Stability", *Journal of American Society*, vol. 129, pp. 15096-15097, 2007.
- [4] Z. Tong and Y. Deng, "Synthesis of Water-Based Polystyrene-Nanoclay Composite Suspension via Miniemulsion Polymerization", *Industrial & Engineering Chemistry Research*, vol. 45, pp. 2641-2645, 2006.
- [45] G. Wu, A. Mikhailovsky, H. Khant, C. Fu, W. Chui and J. Zasadzinski, "Remotely Triggered Liposome Release by Near-Infrared Light Absorption via Hollow Gold Nanoshells" *J. Am. Chem. Soc.*, 130, pp.8175-8177, 2008
- [6] C. A. Coutinho, R. K. Harrinath, V. K. Gupta, "Settling characteristics of composites of PNIPAM microgels and TiO₂ nanoparticles", *Colloids and Surface*, vol. 318, pp. 111-121, 2008.
- [7] D. Nguyen, H. S. Zondanos, J. M. Farrugia, A. K. Serelis, C. H. Such, and B. S. Hawkett, "Pigment Encapsulation by Emulsion Polymerization Using Macro-RAFT Copolymers", *Langmuir*, vol. 24, pp. 2140-2150, 2008.
- [8] N. Peppas, Y. Huang, M. Torres-Lugo, J. Ward, and J. Zhang, "Physicochemical, foundations and structural design of hydrogels in medicine and biology," *Annual Review of Biomedical Engineering*, vol. 2. pp. 9-29, 2000.
- [9] G. T. Franzesi, B. Ni, Y. Ling, and A. Khademhosseini, "A Controlled-Release Strategy for the Generation of Cross-Linked Hydrogel Microstructures", *Journal of American Chemical Society*, vol. 128, pp. 15064-15065, 2006.
- [10] D. Bharali, S. Kumar Sahoo, S. Mozumdar, and A. Maitra. "Cross-linked polyvinylpyrrolidone nanoparticles: a potential carrier for hydrophilic drugs" *Journal of Colloid and Interface Science*, vol. 258, 415-423, 2003.
- [11] N. Peppas, J. Hilt, A. Khademhosseini, and R. Langer "Hydrogels in Biology and Medicine: From Molecular Principles to Bionanotechnology", *Advance Material*, vol. 18, 1345-1360, 2006.

[12] B. Wang, W. Zhu, Y. Zhang, Z. Yang and J. Ding, "Synthesis of a chemically-crosslinked thermo-sensitive hydrogel film and in situ encapsulation of model protein drugs", *Reactive & Functional Polymers*, vol. 66, pp. 509–518, 2006.

[13] W. Hennink and C. van Nostrum, "Novel crosslinking methods to design hydrogels", *Advanced Drug Delivery Reviews*, vol. 54, pp. 13-35, 2002.

[14] N. Peppas, H. Moynihan and L. Lucht, "The structure of highly crosslinked poly(2-hydroxyethyl methacrylate) hydrogels," *Journal of Biomedical Materials Research*, vol. 19, pp. 387 – 410.

[15] N. Peppas, J. Zach, A. Khademhosseini, and R. Langer, "Hydrogels in biology and medicine: from molecular principles to bionanotechnology" *Adv. Mater*, vol.18, pp.1345-1360, 2006.

[16] B. Shenoy, Y. Wang, W. Shan and A. Margolin, "Stability of Crystalline Proteins", vol.73, pp. 358-369, 2000. [10] E. Bourgea-Lami and J. Lang, "Encapsulation of Inorganic Particles by Dispersion Polymerization in Polar Media" *Journal of Colloid and Interface Science*, vol. 197, 293-308, 1998.

3 LITERATURE REVIEW

Particle encapsulation has many variables that play important roles when homogeneous particle dispersion is desired. The literature presents a wide variety of systems for particle encapsulation. They can be created in situ or encapsulated within a membrane. The following discussion presents the most relevant published work regarding particle encapsulation.

Literature reports the encapsulation of various types of particles within different types of substrates. For example, Zhang and colleges studied monodispersed and highly magnetic responsive microspheres with magnetite nanocrystals formed in a polymeric matrix. The particles are created inside the matrix; the iron hydroxide colloids are trapped inside the polymer and converted into magnetite nanocrystals. The method is based on the formation of iron hydroxide/polymer composite microspheres by acid-catalyzed condensation polymerization of urea and formaldehyde in the presence of colloidal iron hydroxide. The iron hydroxide colloids entrapped in the polymer matrix are then in situ converted to magnetite nanocrystals by reaction with sodium borohydride under hydrothermal conditions. Particles with an average diameter $3.8 \pm 0.19 \mu\text{m}$ were obtained. They concluded that the morphology and magnetic properties of the particle products could be controlled through the aspects that affect the polymerization and the reaction. These researchers, however, did not examine the factors involved in the dispersion of particles in the membrane [1].

Particles of poly-(*N*-isopropylacrylamide) (PNiPAM) microgels where encapsulated in polyacrylamide (PAAm) hydrogel matrix by Musch and colleges at different temperatures and cross-linking densities, below and above the volume phase transition temperature of PNiPAM. They demonstrated that the thermosensitive swelling behavior of the PNiPAM microgels is fully retained in the composite material and the temperature collapse or swollen the microgel particles. The radius range was 45-115nm [3].

Another example is by Soulé et al who presented the characterization of polymer particles embedded in a solid polymer matrix. They polymerized a solution of isobornyl methacrylate (IBoMA) in polyisobutylene. These systems experienced a phase separation and spherical micron sized particles of polyisobutylene were formed with

diameters to 0.19 – 0.40 μm . This work demonstrated the possibility of measuring still particles using a one dimensional array of light detectors. Soulé et al did not examine particle distribution within the membrane [2].

Another important aspect to study in particle encapsulation is the interaction between the particle and the membrane. The adhesion between chemically dissimilar solids has been studied by Valadares et al. They worked with different pairs of organic and inorganic nanoparticles: Stöber silica and poly(styrene co-butyl acrylate-co-acrylic acid) (SA) latex, calcium montmorillonite and SA latex, and titanium dioxide with SA latex. Aggregated particle nanohybrids were obtained by drying mixed aqueous dispersions at different particle concentrations. The diameter of silica particles was 169 nm and latex particles were 64nm. They found that stable hybrid aggregates and monoliths were unexpectedly formed upon drying of aqueous dispersions of very different nanosized particles as a result of the formation of stable interfaces between the organic and inorganic phases. For the distribution of the particles, they found that even though the particles in each pair are divergent and thus are expected to have a high interfacial tension adhesion [6].

Particle charge is a significant factor that is part of the interaction between particle and membrane. Interestingly, the literature data about this is limited. The work of Van Tomme and colleagues studied the degradation of dextran hydrogels composed of positively and negatively charged microspheres. Negative charged microspheres (dex)-2 hydroxyethyl methacrylate (HEMA)-methacrylic acid (MAA) and positive charged microspheres (dex)-2 hydroxyethyl methacrylate (HEMA)- dimethylaminoethyl methacrylate. They concluded that increasing the percent of solid and the amount of negatively charged microspheres, showed an increase on the degradation time of the particles. Changing the quantity of positive and negative microspheres also altered the degradation of the hydrogel. The diameter of the particles was 9 μm [7].

Van Tomme and colleagues in 2008 published the effect of size and charge microspheres of dextran-HEMA, in hydrogels. Charged monomers, methacrylic acid (MAA) or N,N-dimethyl aminoethyl methacrylate (DMAEMA) were added to dex-HEMA to create charged particles. The rheological analysis explains that when the surface charge is increased, stronger hydrogels were obtained. Small microspheres with a

diameter smaller 14 μm , produced stronger hydrogels in contrast with larger microspheres from 20 -50 μm . Considering charge and size, the storage moduli (G_0) of fully elastic hydrogels could be adapted from 400 to 30,000 Pa [8].

Different particles had been encapsulated in polymers as magnetic nanocrystals, (PNiPAM) microgels, polyisobutylene and different pairs of organic and inorganic nanoparticles. Literature reports that the interaction between dissimilar solid, particle and membrane, can create highly interfacial adhesion. For the particles, an increase in superficial charge was found to create stronger membranes.

Literature also reported the analysis of the particle dispersion in polymeric membranes. Wassel evaluated the encapsulation of superparamagnetic iron oxide nanoparticles (SPIONs) coated with oleic acid in poly(d,l-lactide-co-glycolide) (PLGA) with an oil-in-water-in-oil emulsion. The SPIONs were evenly distributed in the PLGA particle and the amount of magnetite incorporated was proportional to the amount in the feed. The diameter range was 5-15nm [4].

Sedimentation of suspensions is a significant phenomenon in the homogenous dispersion of particles, Coutinho and his group reported the settling of titanium dioxide nanoparticles embedded in microgels of poly(*N*-isopropylacrylamide). They found that microgel–titania composites showed rapid sedimentation in aqueous dispersions and the settling time decreased as the amount of TiO_2 increases from 10% to 75%, weight. This data was validated by using solid, impermeable silica spheres of two different sizes (3.2 μm and 0.45 μm) which followed Stokes law [5].

Particles distribution has been analyzed in literature according to homogeneity and particles sedimentation, with PLGA particles was created homogenous dispersed membranes and particles sedimentation depends on the concentration of the particles [4, 5]. Literature did not report the physical and chemical factors that can interfere in the homogenous distribution of particles in polymers. Only the work of Van Tomme considered the charged particles of various diameters, but the literature did not describe the dispersion of the particles in the membrane taking into account these factors and further including the effect of substrate charge, size and concentration. These factors are important in order to create a homogeneously dispersed membrane and to guarantee that there is a known concentration in the membrane.

Physicochemical factors are always presents in the interaction of two different compounds. When particles are going to be encapsulated in a membrane several chemical and physical factors most be considered as membrane charge, particle charge, particle concentration and size.

3.1 REFERENCES

- [1] L. Zhang, L. Chen, and Q. Wan “Preparation of Uniform Magnetic Microspheres through Hydrothermal Reduction of Iron Hydroxide Nanoparticles Embedded in a Polymeric Matrix”, *Chemistry of Materials*, vol. 20, pp. 3345–3353, 2008.
- [2] E.. Soulé, Guillermo E. Eliçabe, “Determination of Size Distributions of Concentrated Polymer Particles Embedded in a Solid Polymer Matrix” *Part. Part. Syst. Charact.* vol. 25, pp. 84–91, 2008.
- [3] J. Musch, S. Schneider, P. Lindner, and W. Richtering, “Unperturbed Volume Transition of Thermosensitive Poly-(*N*-isopropylacrylamide) Microgel Particles Embedded in a Hydrogel Matrix”, *Journal of Physical Chemistry*, vol. 112, pp. 6309–6314, 2008.
- [4] R. Wassel, B. Grady, R. Kopke and K. Dormer, “Dispersion of super paramagnetic iron oxide nanoparticles in poly(d,l-lactide-co-glycolide) microparticles”, *Colloids and Surfaces A: Physicochem. Eng. Aspects*, vol. 292, pp. 125–130, 2007.
- [5] C. A. Coutinho, R. K. Harrinath, V. K. Gupta, “Settling characteristics of composites of PNIPAM microgels and TiO₂ nanoparticles”, *Colloids and Surface*, vol. 318, pp. 111-121, 2008
- [6] L. Valadares, E. Linares, F. Bragança, and F. Galembeck, “Electrostatic Adhesion of Nanosized Particles: *The Cohesive Role of Water*, *J. Phys. Chem. C*, vol. 112, pp. 8534–8544, 2008,.
- [7] S. Van Tomme, C. van Nostrum, S. de Smedt and W. Hennink, “ Degradation behavior of dextran hydrogels composed of positively and negatively charged microspheres”, *Biomaterials*, vol. 27, pp. 4141-4148, 2006.
- [8] S. Van Tomme, C. van Nostrum, M. Dijkstra, S. de Smedt and W. Hennink, “Effect of particle size and charge on the network properties of microsphere-based hydrogels”, *European Journal of Pharmaceutics and Biopharmaceutics*, vol. 70, pp. 522–530, 2008.

4 OBJECTIVES

The in depth understanding of the factors involved in the encapsulation of particles within membranes has not been completely understood. The understanding of particle/substrate interactions are of utmost importance to obtain homogenously dispersed membranes, which are important not only in the pharmaceutical field, but in other fields as well. For this purpose, the main goal of this work is the examination of the physicochemical interaction between particles and cross-linked hydrogels networks for the creation of homogenous dispersed membranes. Specifically, it was intended to:

- Define the effect of particle charge, size and concentration.
- Characterize the effect on composition, charge and characteristics of the hydrogel in the homogenous dispersion of particles.
- Describe of the effect of the particle presence in the mechanical properties of the resulting network.

5 FACTORIAL DESIGN

The interactions between the encapsulation shell and the particles could be affected by surface charges which can interfere with particle distribution. For industrial and pharmaceutical applications, encapsulated particles have particular properties including size, charge, and concentration. The work presented herein examined four factors including particle charge, size, concentration and membrane charge. For this purpose, a factorial design was constructed. The creation of a factorial design helps to examine all the possible combinations of the aforementioned variables. This design allows understanding of the interactions between each variable by minimizing the amount of experiments to be performed [1].

To create the factorial design, each variable must have different levels. The first variable, particle size was selected as to have a wide range which included particles of 100 nm, 1 μm and 100 μm diameters. The particles were selected with the three charges, neutral, positive, and negative. The properties of the polymeric membranes were selected as to have three different charges, neutral, positive, and negative. Finally, two concentrations of particles were established, high and low. Table 5.1 resumes the factors and levels that were followed in this study.

According to the aforementioned variables, in this particular case it was necessary to build a mixed-level factorial design. It included three factors with three levels, 3^3 and one factor with two levels, 2^1 , see table 5.2. The three levels for a 3^3 factorial design are named 0, 1 and 2 and for two levels are 0 and 1. First, a 3^3 factorial design was constructed and added to the factorial design 2^1 . The four factors are particles charge, particles size, particles concentration and membrane charge. Particles charge has three levels, 0 represent positive, 1 is negative and 2 is neutral charge. Particles size presents three levels, 0 is 100 nm of diameter, 1 is 1 μm and 2 is 100 μm . Particles concentration has two levels 0 is low concentration and 1 is high concentration. Finally, membrane charge has three levels, 0 is positive, 1 is negative and 2 is neutral charge. The number one of the table 5.2 represents membranes with positive particles charge, positive membrane charge, 100 nm particle diameter and low concentration and the number 17 represents negative particles charge, neutral membrane charge, 1 μm

particles diameter and low concentration of particles. This applied for the other rows in the table 5.2.

All the synthesized membranes were analyzed for the particle dispersion. From this analysis it was determined if there was a homogenous or heterogeneous distribution. Scanning electron microscopy, near infrared microscopy and rheology were used to achieve the proposed objectives.

Table 5.1. Four Factors of the design

	Particle charge	Membrane Charge	Diameter Particles	Concentration
0	+	+	100 nm	Low
1	-	-	1 μ m	High
2	Neutral	Neutral	100 μ m	

Table 5.2. Factorial Design

	Particle charge	Membrane Charge	Diameter Particles	Concentration
	0: positive	0: positive	0: 100 nm	0: 2.2 w/w %
	1: negative	1: negative	1: 1 μm	1: 4.4 w/w%
	2: neutral	2: neutral	2: 100 μm	
1	0	0	0	0
2	1	0	0	0
3	2	0	0	0
4	0	1	0	0
5	1	1	0	0
6	2	1	0	0
7	0	2	0	0
8	1	2	0	0
9	2	2	0	0
10	0	0	1	0
11	1	0	1	0
12	2	0	1	0
13	0	1	1	0
14	1	1	1	0
15	2	1	1	0
16	0	2	1	0
17	1	2	1	0
18	2	2	1	0
19	0	0	2	0
20	1	0	2	0
21	2	0	2	0
22	0	1	2	0
23	1	1	2	0
24	2	1	2	0

25	0	2	2	0
26	1	2	2	0
27	2	2	2	0
28	0	0	0	2
29	1	0	0	2
30	2	0	0	2
31	0	1	0	2
32	1	1	0	2
33	2	1	0	2
34	0	2	0	2
35	1	2	0	2
36	2	2	0	2
37	0	0	1	2
38	1	0	1	2
39	2	0	1	2
40	0	1	1	2
41	1	1	1	2
42	2	1	1	2
43	0	2	1	2
44	1	2	1	2
45	2	2	1	2
46	0	0	2	2
47	1	0	2	2
48	2	0	2	2
49	0	1	2	2
50	1	1	2	2
51	2	1	2	2
52	0	2	2	2
53	1	2	2	2
54	2	2	2	2

5.1 REFERENCES

[1] D. Montgomery and G. Runger, *Applied Statistics and Probability for Engineers*, Wiley, 1994.

6 Qualitative and Quantitative Determination of Particle Distribution Within Hydrogel Membranes.

6.1 Background

In the past years, infrared (IR), near-infrared (NIR) and Raman spectroscopy have been used in different analysis of pharmaceutical products. Infrared (IR) and near-infrared (NIR) are based on vibration spectroscopy and reveal physical and chemical mechanisms at the molecular level. Raman spectroscopy reveals only chemical information. For pharmaceutical processes the understanding of such mechanisms is of utmost importance for quality control [1].

Chemical imaging is an innovative technique that uses conventional imaging and spectroscopy to obtain spatial and spectral information from a sample. Near infrared chemical imaging (NIR-CI) unites the chemical selectivity of vibrational spectroscopy and the potential of image visualization. Additionally is a multidisciplinary technique that combines two important aspects, spectroscopy, and signal and image processing [2]. The combination of both aspects creates a more complete instrument which can be applied for the determination of ingredient distribution in solids, semi-solids, powders, suspension and liquids [3].

Specifically, chemical imaging is the arrangement of microscopes and vibrational spectrometers to create a 2D image of a sample. Ideally, it shows a mapping or true image of the components of the analyzed sample based on their chemical composition and spatial location [4]. Each pixel contains a spectrum in that position. The image is a three-dimensional block of data with two spatial and one wavelength dimension, see Figure 6.1 [3]. This block is called a hypercube. One acquisition stores thousands of images across different wavelengths. A single image plane illustrates the absorbance of the sample at a particular wavelength [5].

A three dimensional image can be constructed by two methods. The first is known as pushbroom acquisition [3]. In this particular method simultaneous spectral

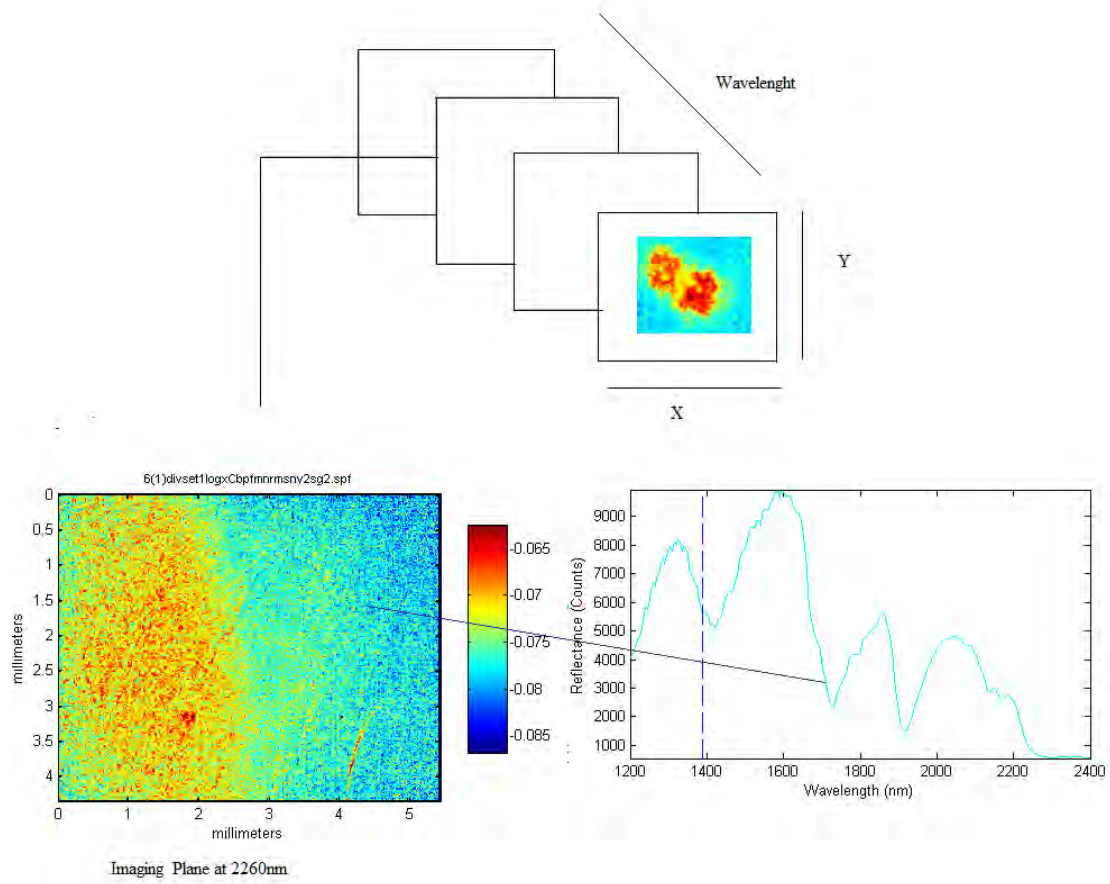


Figure 6.1 Near infrared chemical imaging hypercube.

measurements are taken from series of nearby spatial positions and the sample is moved underneath the instrument. This technique has been applied with Raman. The advantage of this technique is that it is able to take the spectra of the entire sample without touching it or moving it manually. The second technique, known as staring imaging, the configuration of the instrument keeps the view of the image fixed and the images are taken one wavelength after another. Near infrared chemical imaging (NIR-CI) is an example of this [3]. The main advantage of this method is that it does not require moving parts.

In this investigation near infrared chemical imaging is chosen as a technique of analysis. It is a non destructive technique and in a few minutes can take a large number of spatial spectra data [6]. NIR is a staring imaging, has been used principally for material characterization and to evaluate sample heterogeneity and the distribution of the chemical components.

6.2 Spatial sample distribution with near infrared chemical

NIR spectroscopy has been used in several applications in the pharmaceutical industry because it offers excellent quality information and reliability of sampling. An important problem in pharmaceutical industry is that distribution of the ingredients in the tablet can alter the performance of a formulation. Agglomeration is commonly observed in classic solid dosages [5]. This section discusses the application of NIR in the study of homogeneity in pharmaceutical tablets.

Awa and colleagues studied self-modeling curve resolution (SMCR) for NIR imaging of pharmaceutical tablets containing pentoxifylline (PTX) as active ingredient and palmitic acid as an insoluble excipient. Ten grams of PTX and 40 g of palmitic acid were ground for 0, 0.5, 1, 2, 10 and 45 min with 250 rpm rotating speed. NIR spectra were taken in $400\ \mu\text{m} \times 400\ \mu\text{m}$ samples with a special resolution of $25\ \mu\text{m}^{-1}$ pixel. The study found that homogeneity depended on the grinding time. Also, the variation in active ingredient distribution also affected the release rate of PTX from the tablet. They concluded that NIR imaging and SMCR combined created a powerful and versatile tool

to understand the chemical and physical mechanism made by the manufacturing process of pharmaceutical products [1].

As it can be expected, the instrument provides a significant amount of information that must be interpreted. In particular, if the distribution of a molecule is intended, spectral data must be deconvoluted to obtain the required information. Chan and colleagues studied the spatial distribution of compacted pharmaceutical tablets and the chemical imaging technique employed was combining *in situ* Attenuated Total Reflexion (ATR) approach and Fourier Transformed Infrared (FTIR) imaging. The research proves that this method can help to study tablet compaction. The spatial distribution was examined comparing the absorbance distribution in histogram of pure Hydroxypropylmethylcellulose (HPMC) and HPMC with 5 wt% magnesium stearate (MgS). The histograms presented a normal distribution with similar peaks concluding that the addition of MgS did not have a strong effect on the density distribution. Pure HPMC had a standard deviation of 0.0355 and with 5 wt% MgS of 0.0404. However, the histogram for the sample with 5 wt% of MgS shifted to a higher integral value indicative of a higher HPMC density [7].

Another method used to describe particle distribution was described by Hilden et al. They studied how the particle size of the extra-granular tartaric acid affects the uniformity of its distribution within BMS-561389 (Razaxaban) tablets. They acquired near chemical infrared spectra to the surface top and bottom of the tablets to assess the distribution of tartaric acid. The images were pre-processed and a principal component analysis was done. The second principal component was more related to the difference between the tartaric acid spectrum and the excipient spectrum. A contour delineation was chosen which allowed the selection of a threshold and the creation of a binary image showing the pixels above and below the threshold. The chemical image analysis outcomes indicated that separation of tartaric acid between tablet tops and bottoms was significant in tablet lots containing large and intermediate sizes, but for tablets with small particle sizes the difference was not significant [8].

In addition to pharmaceutical mixtures NIR can be used in a wide variety of materials. Furukama et al. described the evaluation of polymers blends with NIR. Poly(*R*-3-hydroxybutyrate) (PHB) and poly(L-lactic acid) (PLLA) were mixed at different ranges from 20 to 80% to study the quality of the blends with the NIR. The qualitative and quantitative analysis concluded that the PHB/PLLA blends were homogenous. Qualitatively, the color gray presented by the score images, the intermediate between black and white, and quantitatively the small standard deviation reported by the histograms at the intensity of the scores images [9].

Chemical imaging had been used to investigate the homogeneity of pharmaceutical tablets, according to the grinding time, compaction and comparing the bottom and top of a tablet. Blend of polymers had also been studied to observe its homogeneity quantitative and qualitatively. Therefore, NIR is a versatile technique that promises to provide enough information regarding the study of particle distribution in polymeric gels and can provide the means to explain the factors involved in particle distribution within membranes. Other techniques such as scanning electron microscopy only provides qualitative information of a really small area, but NIR can provide qualitative as well as quantitative data of a significantly bigger area.

6.3 Materials and methods

6.3.1 Hydrogel preparation

The hydrogels were prepared by free radical polymerization. Different monomers were employed anionic: methacrylic acid (MAA), cationic, (N,N-dimethyl amino) ethyl methacrylate (DMAEM), and neutral: 2-hydroxyethyl methacrylate (HEMA). The crosslinker was poly(ethylene glycol) dimethacrylate (PEGDMA 1000) (n=1000) (PolySciences Inc. Warrington, PA). A solution 1:1 v/v deionized water/ethanol (Fisher Scientific, Pittsburgh, PA) was used as the diluents. The particles were silica: plain, aminated and carboxylated with 100nm, 1 μ m and 100 μ m diameters from (Corpuscular, Cold Spring, NY). The UV initiator was 2-hydroxycyclohexyl phenyl ketone (Sigma-

Aldrich, Milwaukee, WI). Hydrochloric acid 6 N and sodium hydroxide 5 M was used to change the pH of the pre-polymeric solution.

Monomer, crosslinker and diluents were weighed in amber bottles with septum screw caps, according to concentration from table 6.1. The particles were added after the pre-polymeric solution was sonicated and a homogenous mixture was observed. The initiator was added and the mixture was again sonicated and placed in an inert glove box (Cole-Parmer Instrument Co., Vernon Hills, IL). The mixer was bubbled with nitrogen for 20 minutes. Bubbles were eliminated to facilitate a homogeneous polymerization leaving the solution rest for five minutes. The mixture was poured by capillarity between two microscope slides separated by Teflon spacers of 0.30 inch thick and irradiated with UV radiation from a mercury lamp as the ultraviolet light source (EXFOS Lite, Mississauga, Ontario) under nitrogen atmosphere for a specific 5 minutes for MAA, 10 minutes for DMAEM and 15 minutes for HEMA.

6.3.2 Zeta Potential

The net charge of the silica particles was studied with dynamic light scattering by using BI-90 Plus Particle Size Analyzer and Zeta Potential Analyzer (Brookhaven Instruments Corporation, Holtsville, NY). Particle suspension was diluted with dionized water until a clear suspension was observed. KNO_3 was added to the suspension such that the salt concentration in it was 1 mM to keep the conductivity constant. The solution pH was changed from 2.0 to 10.0 with KOH and HNO_3 solutions with concentration of 0.1 N and 0.001 N, respectively. Zeta potential for plain, aminated and carboxylated particles was determined.

6.3.3 Scanning Electron Microscopy

Hydrogels were placed in ethanol for at least 12 hours. Hydrogels were cut with a razor blade and dried by the technique known as critical point drying. Samples are coated with gold and observed under scanning electron microscope. The top and cross-

Table 6.1 Hydrogel composition.

Membrane Negative		
MAA: PEGDMA	88:12	%Molar
Diluent	60	%Molar
Membrane Positive		
DMAEM: PEGDMA	83.2:16.8	%Molar
Diluent	60	%Molar
Membrane Neutral		
HEMA:PEGDMA	99.4:0.6	%Molar
Diluent	40	%Volume

sectional membrane areas were observed. This technique allowed a qualitative observation of the distribution of the particles inside the membrane.

6.3.4 Near infrared chemical imaging

The near infrared chemical imaging was performed using a SyNIRgi™ NIR Spectral Imaging System (Spectral Dimensions, Inc, Olney, MD). The imaging system consists of a liquid crystal tunable filter (LCTF) coupled with an NIR sensitive Focal Plane Array (FPA) detector. The diffuse reflectance image of the sample is passed through the LCTF, which provided a spatial resolution of 320*256 pixels. The size of each pixel is 17.5X17.5 μm, giving an imaging area of 4.35*5.44 mm. The spectrum is measured with 1 scan, in a spectral range of 1200 to 2450 nm, each 10 nm steps. The data collected was processed using ISys® software. Three membrane areas were scanned with the NIR.

After the data from near chemical imaging was acquired, it was preprocessed using ISys® software. First, a background correction was performed. Followed by removal of bad pixels, normalization was performed, standard normal variation, and finally a second derivative with 9 points and 3rd grade polynomial.

6.4 Results

6.4.1 Zeta Potential

Solid surfaces can become charged in liquid due to the differential solubility, direct ionization of surface group and specific ion absorption. Surface charge produces electrostatic repulsion between particles and creates stable colloidal dispersions. Zeta potential is the difference in the electrostatic potential between an average point in the shear plane (plane where the liquid and charges move with the colloidal particles) and one far out in the liquid. [9].

Zeta potential depends on the particle charge and the concentration of free salt ions. The solution pH modifies the zeta potential of the particle. The neutral, positive and

negative monomers have specific pHs. MAA that has a carboxyl group, see figure 6.2 and in the pre-polymeric solution has an acidic pH, see table 6.2. DMAEM has an amino group, see figure 6.2 and in the pre-polymeric solution has a basic pH, see table 6.2. HEMA does not have any functional groups and have an acid pH in the pre-polymeric solution, see table 6.2. Functionalized silica has an amino group for positively charge and a carboxyl group for negatively charged particles, see figure 6.3.

When the silica particle is placed in contact with the pre polymeric solution the zeta potential varies. This is a relevant factor since the surface charge of the particles needs to be positive, negative or neutral. The particle suspension pH was changed from 2.0 to 10.0 to determine the isoelectric pH, as shown in figure 6.4. Results of the isoelectric point are summarized in table 6.3

The lowest isoelectric pH was for the particles without any functionalized group, followed by the carboxylated, and, finally, the aminated. The higher the magnitude of the zeta potential the particle dispersion is expected to become more stable. If particles have a zeta potential higher than +30mV or lower than -30mV the dispersion is said to be stable [9]. The silica particles without any functional group have a zeta potential between +15mV and -30mV, therefore the particles do not have any force that prevents their agglomeration because they do not repel or attract each other. These particles were used as neutral charge particles and the pH of the pre-polymeric solution was changed to values near the pI of neutral particles which is a value of 3.5. For carboxyl functionalized particles the zeta potential goes from +45mV to -30mV from low to high pH respectively, so the particles at pH higher than 4.5 must repel from each other and had negative charge. The amine functionalized particles present values of zeta potential from +45mV to -45mV, so the particles at pH lower than 8.0 must repel from each other and have positive charge.

The pre-polymeric solution pH was modified to values according each type of particle. For positive particles (amine particles) the prepolymeric solution pH was not modified.

Table 6.2 Monomer solution pH and pKa

Particle	pH	pKa
HEMA	4.6	
MAA	3.2	4.66
DMAEM	9.2	8.44

Table 6.3 pI silica particles

Particle	pI
Neutral	3.5
Negative	4.5
Positive	8.0

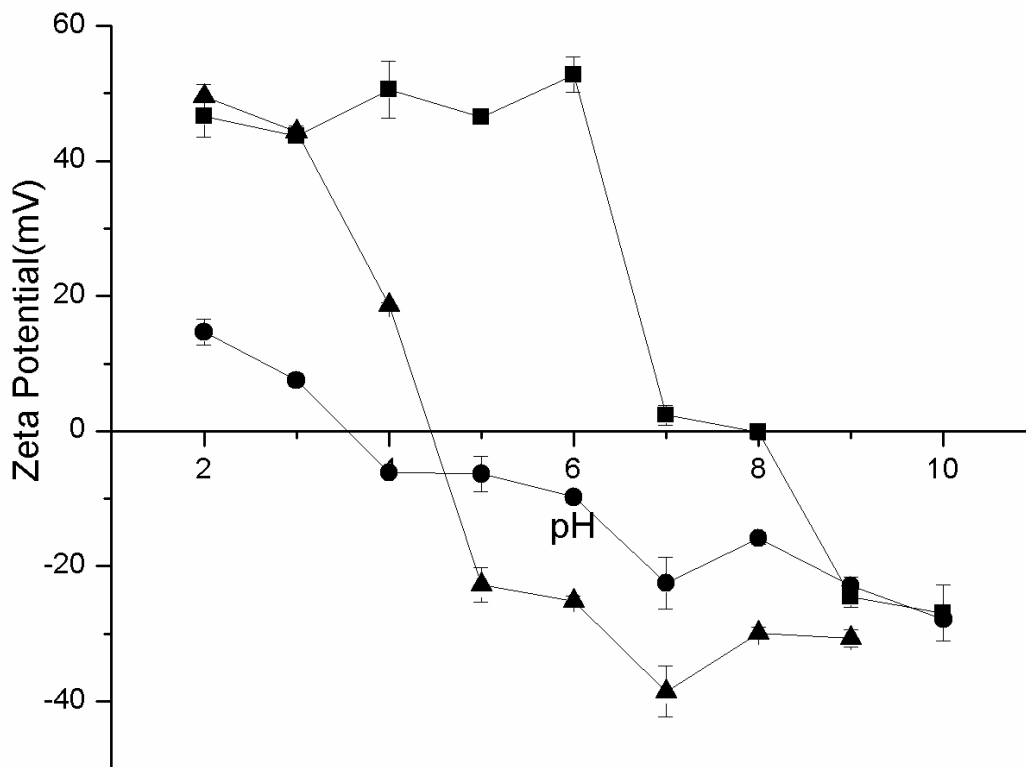


Figure 6.4 Zeta Potential for functionalized silica particles at various pH's. ● unfunctionalized silica, ▲ silica with carboxyl groups and ■ silica with amine groups.

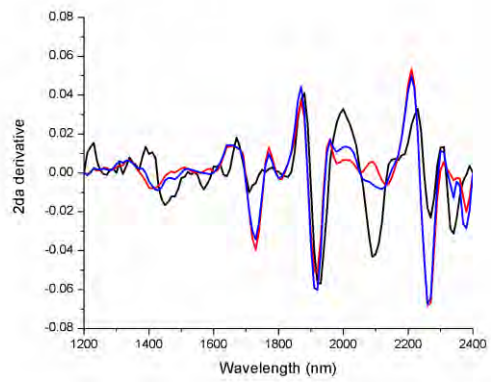
For negative particles (carboxylated particles) the prepolymeric solution pH was modified only for MAA and HEMA. For neutral particles the MAA and HEMA prepolymeric solution pH was change to 3.5, but for DMAEM was used amine particles, because DMAEM is a strong base and the pre-polymeric solution cannot be dilute with an acid. on pH was modified to values lower than the pI for aminated particles 8.0.

6.4.2 Near infrared chemical imaging

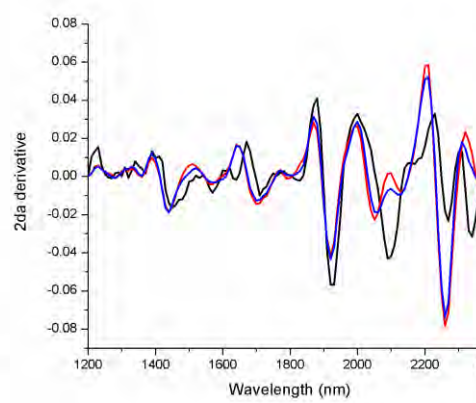
6.4.2.1 NIR qualitative inspection of particle distribution

Near infrared chemical imaging (NIR-CI) is a technique that allows gathering spatial and spectral information from a sample [2]. NIR can also show the localization of particles in a membrane, help to understand the distribution of silica particles in the hydrogels and define the homogenous or heterogeneous particle distribution qualitatively and quantitatively. Other techniques, such as SEM, only give a qualitative image of a small area.

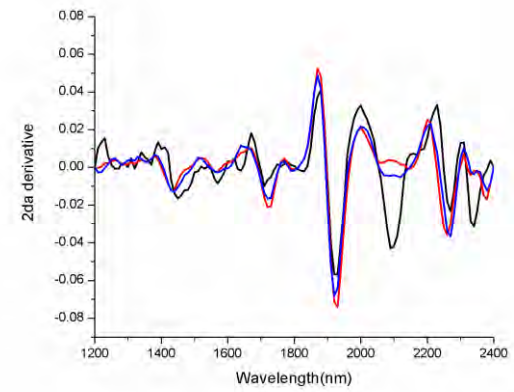
The first step was to determine if the NIR reflectance penetrated the hydrogel completely. A paper napkin was used as background. The paper napkin has a different band from the hydrogel at 2100 nm (Figure 6.5). The napkin was placed below each of the hydrogel membranes with silica particles encapsulated and several images were taken. Figure 6.5 shows the spectra from the hydrogels, the napkin and the napkin below the hydrogel for DMAEM, HEMA and MAA. A second derivative was calculated so the chemical bands are minimum peaks that correspond to maximum points in the spectrum.



a)



b)



c)

Figure 6. 5 Spectra for a) DMAEM b) HEMA, c) MAA to show NIR penetration. (—) napkin spectrum. (—) hydrogel spectrum. (—) hydrogel with napkin underneath.

The spectra from the DMAEM and MAA hydrogels with a napkin below shows that a new band is formed in the hydrogel spectrum at 2100 nm, therefore the NIR is able to penetrate the hydrogel, because the NIR ray is going through the hydrogel, touching the napkin and reflecting it. HEMA has a different behavior since spectrum did not present a band at 2100 nm, but the width of the HEMA band at 2150 nm grew (see figure 6.5 b)) showing how the napkin affect the NIR bands. Particles dispersion studies need to evaluate the complete irradiated area and not only the top to understand completely the particles behavior.

The second step was to determine if the NIR was capable of identifying the differences between the polymer and the silica particles when the silica is encapsulated in the polymer. For this purpose, various images of the proposed hydrogels were obtained using the NIR. The NIR takes images from wavelengths of 1200 nm to 2450 nm, so from each selected band there is a chemical image. The hydrogel is composed of different chemicals which possess a variety of NIR bands, so it is important to understand in which bands the silica particles, the polymer and other chemicals are observed in the NIR.

Figure 6.6 show the spectrum from each hydrogel with and without particles. The spectrum belongs to hydrogels with encapsulated particles of 100 μm . The principal bands for DMAEM, HEMA and MAA are located at 1400, 1730, 1920 and 2260 nm. The chemical change between the system with and without particles is not significant, but subtle differences are observed. The hydrogel spectrum is stronger than the silica spectrum. Most of the variability is from concentration in some of the bands, such as for DMAEM at 2260 nm where the band decreases its intensity when the particles are added.

The several bands presented in the spectrum of the hydrogels represent different chemical bonds, so it is imperative to understand the chemical meaning of each of the bands. The silica-hydrogel system has chemical important structures that must be studied, such as the silica, the hydrogel and water. Water is important because hydrogel and silica are hydrophilic materials. Each molecule mentioned above was

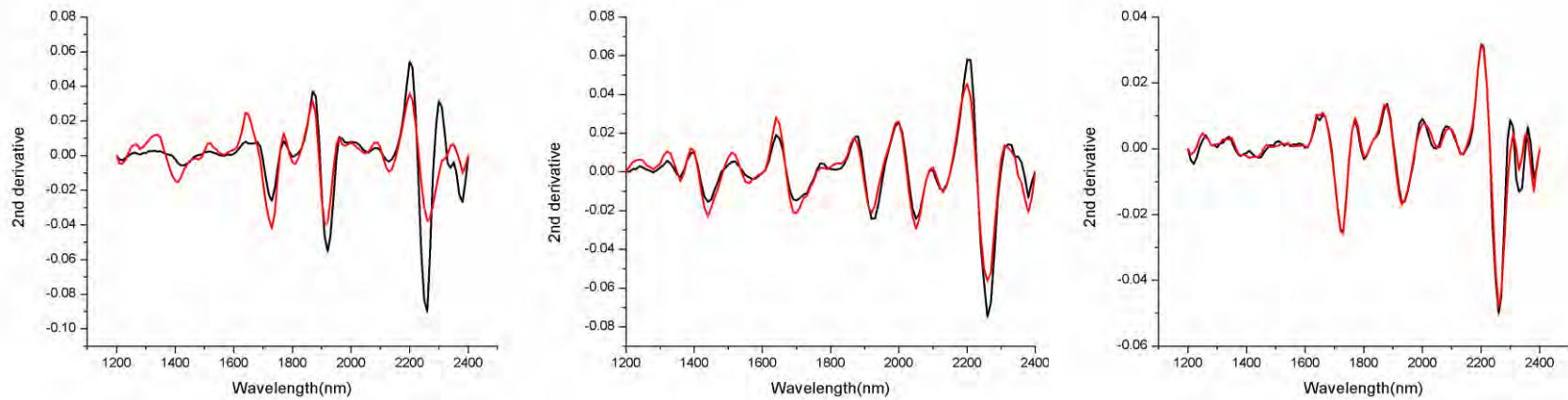


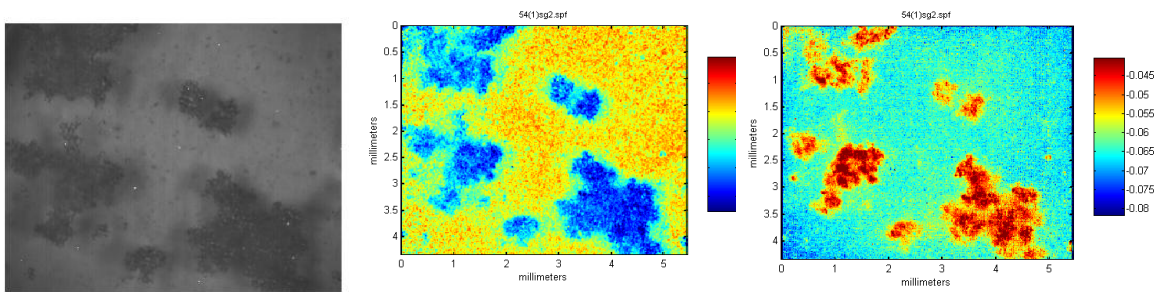
Figure 6.6 a) DMAEM NIR spectra with and without particles, b) HEMA NIR spectra with and without particles, c) MAA NIR spectra with and without particle. (—) hydrogel without silica particles. (—) hydrogels with silica particles encapsulated.

analyzed and the one with more chemical spatial distribution was chosen.

The first studied band was the one from the silica. Synthetic glass forming and commercial glass have water as an inevitable impurity [10]. Water breaks the Si-O-Si bridges and creates the silanol group 2Si-O-H that affects the NIR transmission [10, 11]. NIR spectrum from silica present two important bands that are designated to the deformation and stretching vibrations of absorbed water molecules [9]. The first overtone of OH in silica is above 1390 nm. Stone and Walrafen defined combination bands in 2240, 2250 and 2210 nm that include an OH stretch with one of the central SiO_2 [11].

The silica and the hydrogels have bands near 1400 nm and between 2240 and 2260 nm, see Figure 6.6. Figure 6.7 shows how the 100 μm particles in DMAEM hydrogel can be detected by the NIR at the two silica bands, 1390 and 2260 nm. Figure 6.7a illustrate silica particles in DMAEM with our conventional microscopy and figure 6.7b and c show the chemical imaging of the same area at 1390 nm and at 2260nm. Notice that the chemical image (figure 6.7b), presents a blue color in the area were particles are expected and a yellow color in area where the polymer is expected. Figure 6.7c has a red color in the area where the particles are expected and a light blue color in the polymer area. In the chemical imaging red color represents the high absorbance area and the blue color the low absorbance area. Similar results were obtained for the rest of the polymer combinations (See Appendix 1). This indicated that the NIR is able to locate the area where the silica particles are at the silanol wavelength, but it is necessary to identify the images changes through the different wavelengths.

The second band to analyze is the NIR band for the C-H bond for aliphatic hydrocarbons that is located between 1700 and 1800 nm [11]. For MAA, DMAEM and HEMA it was observed is the one at 1730 nm, refers to Figure 6.6. This band is not present in silica particles, it is only for the polymers. C-H bond is present in the monomer and crosslinker of the hydrogels as shown in Figure 6.2. Figure 6.8 shows the chemical imaging at 1730 nm and the conventional microscopy image for the three studied hydrogels. For MAA



a)

b)

c)

Figure 6. 7 DMAEM hydrogel with negative 100 μm particles, (a) Conventional microscopy image, (b) NIR chemical imaging at 1390 nm and (c) NIR chemical imaging 2260 nm.

and DMAEM the clusters are not easily discriminated (Figure 6.8). The conventional image and for HEMA are represented by blue color that represents low absorbance. The chemical imaging at the C-H band is a wavelength for the polymer and really weak for silica bonds. In conclusion the C-H band does not describe the area where the particles are located for all hydrogels in the chemical imaging according to the microscopy image

The third band to study is the one from water. Hydrogels are hydrophilic networks and in chemical analysis water can be present and interfere with the results. Silica, as previously mentioned present water as an impurity as well. Weber and Lo defined two NIR bands for water one at 1450 nm and the other at 1940 nm [8]. Figure 6.6 presents the only band near 1940 nm is at 1920 nm and the one of 1450 nm is not detected.

Water was studied placing the silica particles on top of the hydrogels and compared with the particles encapsulated inside the hydrogel. Figure 6.9 presents the chemical imaging and the conventional imaging of encapsulated silica particles and not encapsulated silica particles at 1920 nm. Not encapsulated silica presents high absorbance (red color) in the areas where the silica particles are located. The high absorbance in the silica particles is due to the fact silica is hydrophilic and absorbed water from the atmosphere. When the silica particles are encapsulated in the three hydrogels, the red areas in the chemical imaging are not the areas where the silica particles are located, according to the conventional microscopy image. The water absorption in silica is not strong enough to be observed through the polymer as not encapsulated silica figures, but helps to understand that in this band the silica particles are not observed. The 1920 nm band does not describe the silica particles inside the polymer that is the main objective.

Silica, polymer and water showed different chemical images at the different wavelengths. Silica bands at 1390 nm and 2260 nm the NIR chemical images showed where the particles are located in the hydrogel. The carbon – hydrogen bond at 1730 nm presented the different polymers and it's a wavelength weak for silica particles. Water band did not describe the silica particles inside the polymer even silica is a hydrophilic

C-H

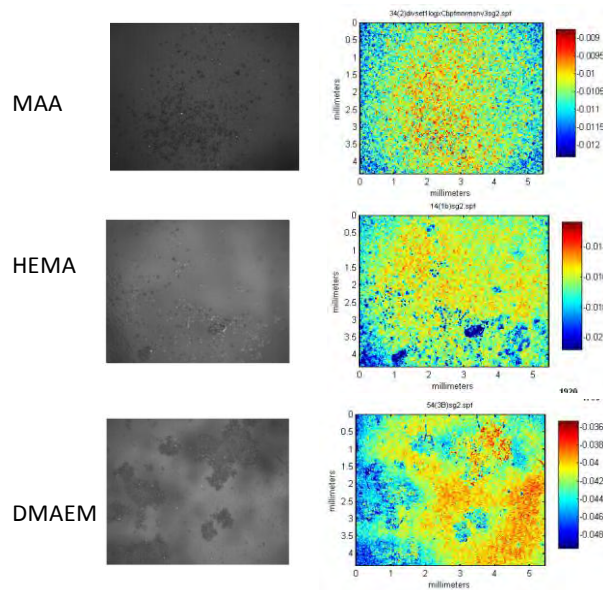


Figure 6. 8 NIR chemical imaging for carbon –hydrogen bond at 1730 nm. Conventional microscopy and NIR chemical imaging

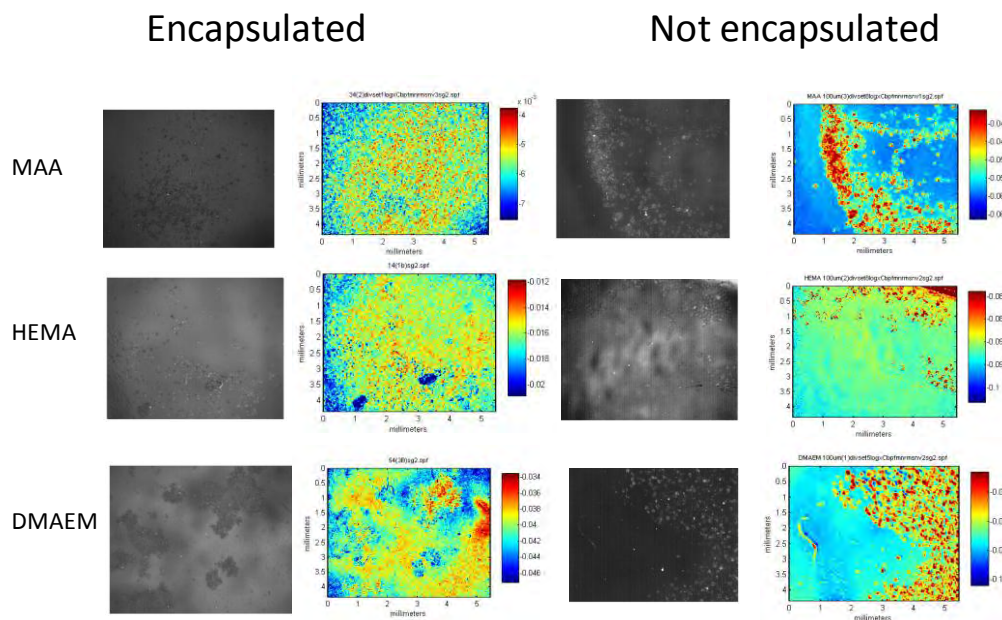


Figure 6. 9 NIR chemical imaging water band 1920 nm for encapsulated and non-encapsulated particles

material. Silica bands are the ones that appeared more reliable in order to study the particle distribution because at 2260 nm the images showed the silica particles in the hydrogels and this is a representative wavelength for silanol bonds. Only these wavelengths are used to study the distribution of particles.

The main objective of this investigation is to understand the distribution of particles in polymeric membranes according to particle size, charge and concentration and membrane charge. All the membranes presented in the factorial design were analyzed with the NIR and to start the propose objective a qualitative study is done with the NIR chemical imaging and the selected wavelengths.

First, it is important to qualitatively study for the distribution of particles with the silica bands. The 100 μm particles are the first to be analyzed. SEM and NIR were used to describe qualitatively the silica particles distribution in each hydrogel. The NIR bands are the silica at 1390 nm and 2260 nm.

Positive hydrogels NIR chemical image and SEM image are shown in figure 6.10 for low concentration and figure 6.11 for high concentration with 100 μm particles. Chemical image for low concentration, figure 6.10, shows that the most uneven distribution is assigned to negative particles. For high concentration, figure 6.11, the most uneven distribution is assigned to negative particles. Both wavelengths for hydrogel DMAEM present similar image, the only different is with neutral particles and high concentration when the wavelength is change to 2260 nm.

SEM images show a qualitative particles distribution of hydrogel. SEM images are not from the same area of NIR images and a smaller area was used. SEM shows how particles are encapsulated and located inside the polymer. No bigger clusters are illustrated by SEM images, because the visual area is not large enough to be able to conclude about clusters.

Neutral membranes NIR chemical image and SEM image are shown in figure 6.12 for low concentration and 6.13 for high concentration with 100 μm particles. Chemical imaging for low concentration, figure 6.12, explains that the most uneven

distribution is assigned to neutral and positive particles. For high concentration, figure 6.13, the one with agglomeration of particles is with positive particles. SEM images shows how particles are covered by the polymer, but still are observed. SEM area is small to study particles aggregation, even though it is easy to see areas free of particles in some membranes.

Negative membranes NIR chemical image and SEM image are shown in figure 6.14 for low concentration and 6.15 for high concentration. Chemical imaging for low concentration, figure 6.14, shows how the membrane with negative particles has the bigger cluster and with high concentration the membrane with neutral particles has an important aggregation of particles visible only at 2260nm. SEM images show highly aggregation in some of the membranes.

When NIR chemical imaging of positive, neutral and negative membranes are compared the one with the biggest clusters is observed in the positive membrane (figure 6.10 and 6.11), followed by the negative membranes (figure 6.14 and 6.15) and finally the neutral membranes (figure 6.12 and 6.13). NIR Chemical analysis shows qualitatively how ionic membranes created bigger clusters in contrast with neutral membrane where clusters were smaller no matter where the particle charge is.

The formation of clusters can be explained by several factors. The silica particles are denser than the pre-polymeric solution so the particles sediment due to the gravitational force generating clusters while polymerization reaction is running. Silica density is 2.65 g/cm^3 and the density of the monomers is 0.93 g/cm^3 for DMAEM, 1.07 g/cm^3 for HEMA and 1.02 g/cm^3 and for MAA. Chemical images showed different distribution for the three types of hydrogels. Neutral membranes have the more homogeneous particles distribution compared with positive and negative membranes. Neutral hydrogels do not have any ion or functional group that interact with neutral, positive and negative particles when are encapsulated, therefore identical charged particles present electrostatic repulsion between them. The particles dispersed along the matrix and created fewer clusters.

Negative and positive membranes had a different behavior. Chemical imaging showed aggregation of particles in both hydrogels for all the particle charges. The attraction between identically charged particles was not expected, but Feng et al. reported that the attraction between ions of the same kind had been observed since some time ago [13].

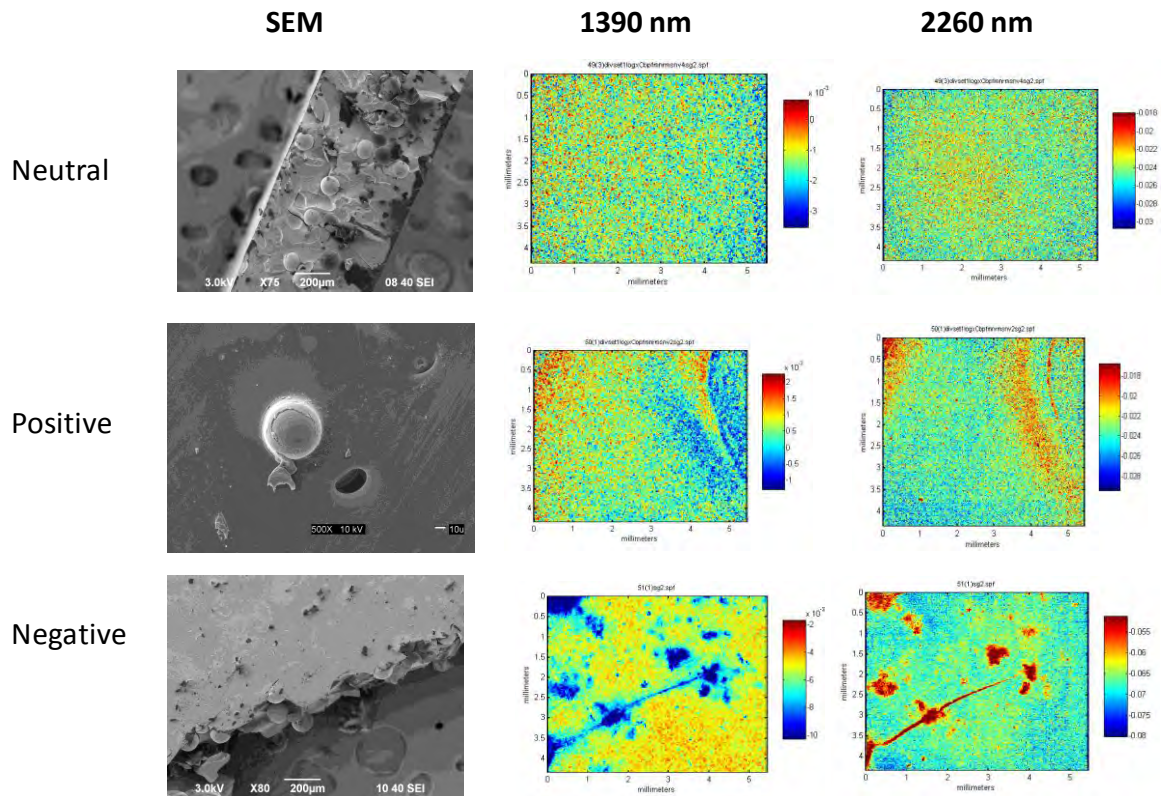


Figure 6. 10 NIR Chemical image and SEM for membrane positive with 100 µm silica particles and low concentration (2.2w/w%) with different charges.

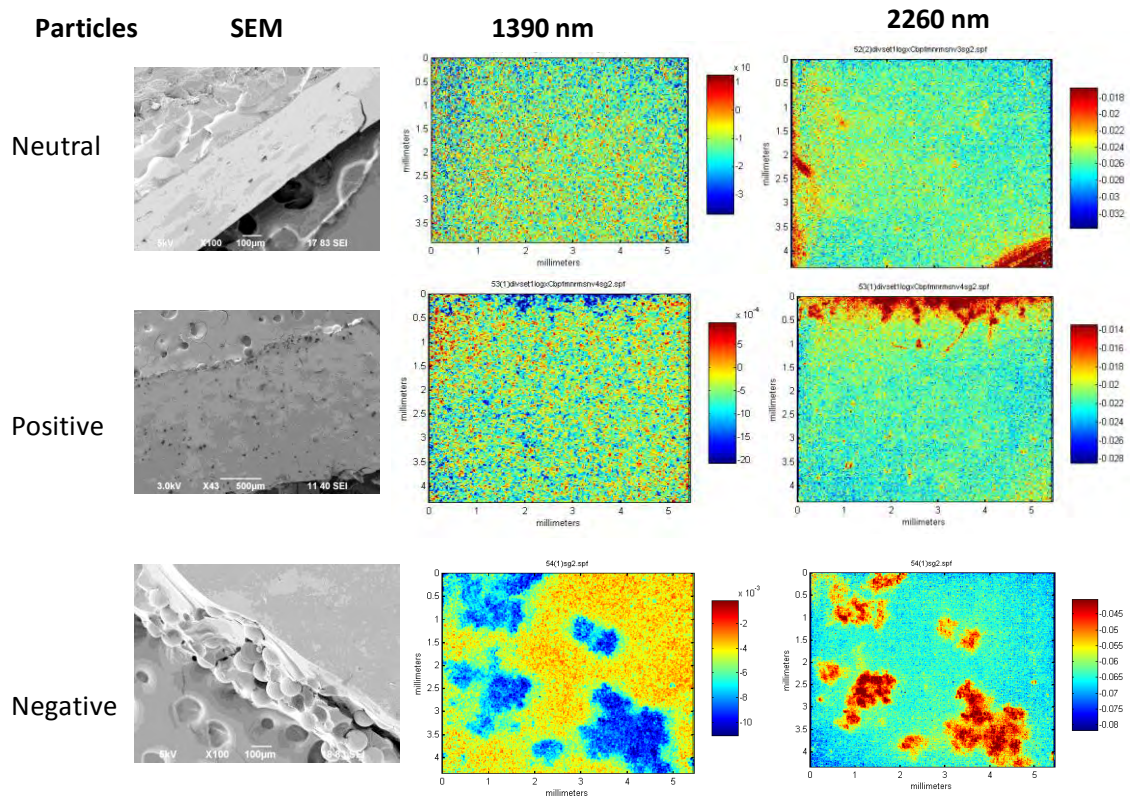


Figure 6. 11NIR Chemical image and SEM membrane positive with 100 µm silica particles and high concentration (4.4 w/w%) with different charges

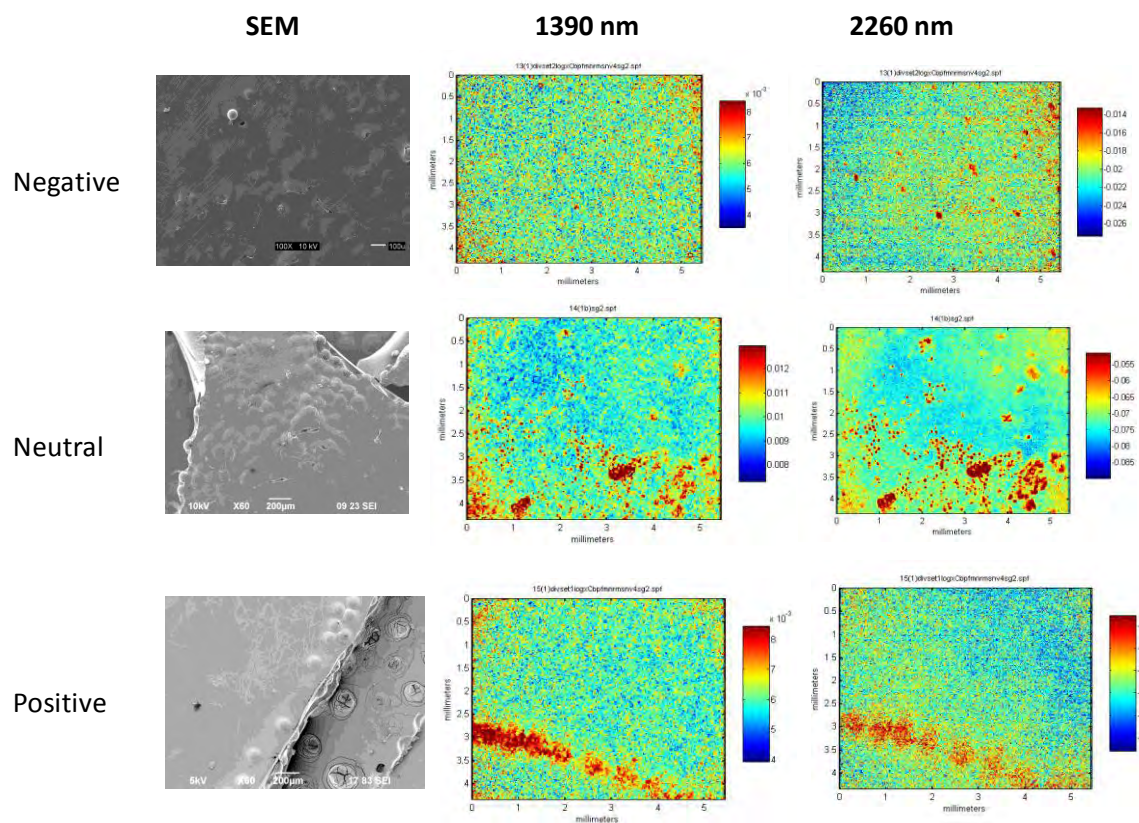


Figure 6. 12 NIR Chemical at 1390nm and SEM membrane neutral with 100 µm silica particles and low concentration (2.2w/w%) with different charges.

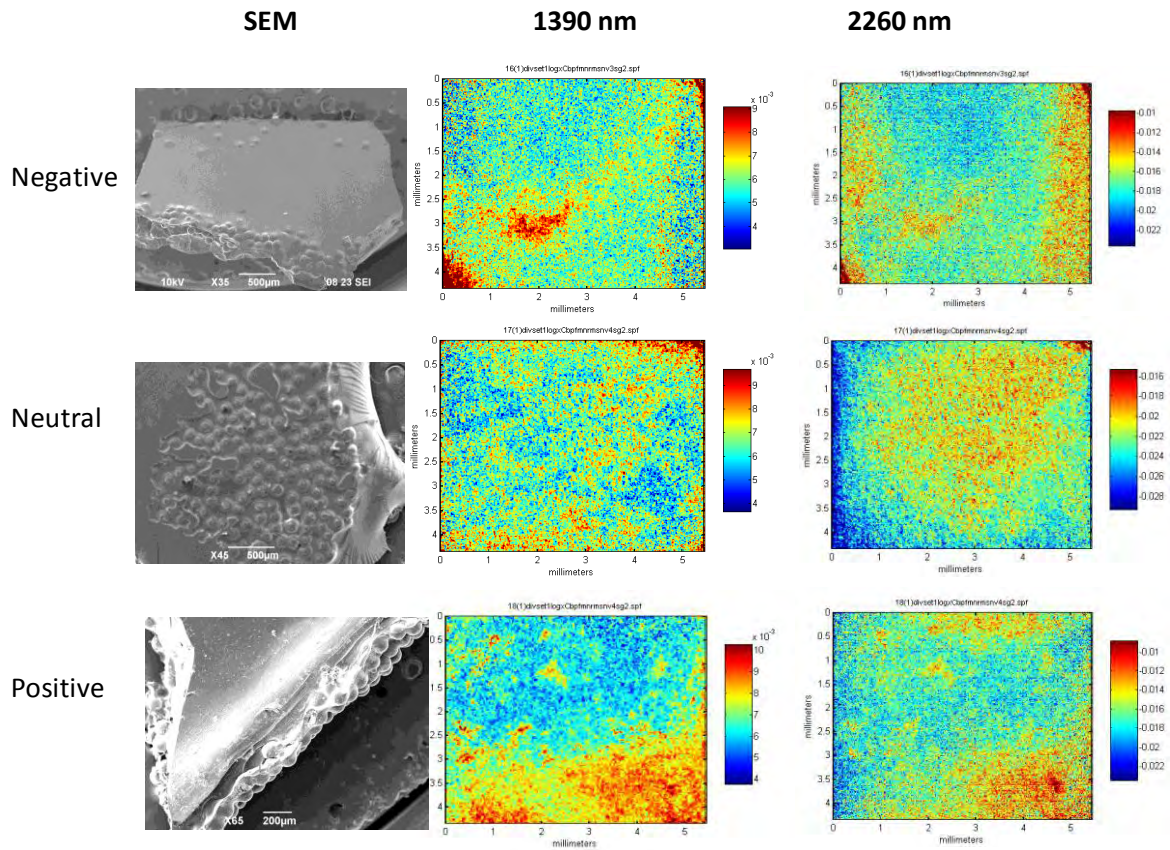


Figure 6. 13NIR Chemical image and SEM images for neutral membrane with 100 µm silica particles and high concentration (4.4 w/w%) with different charges.

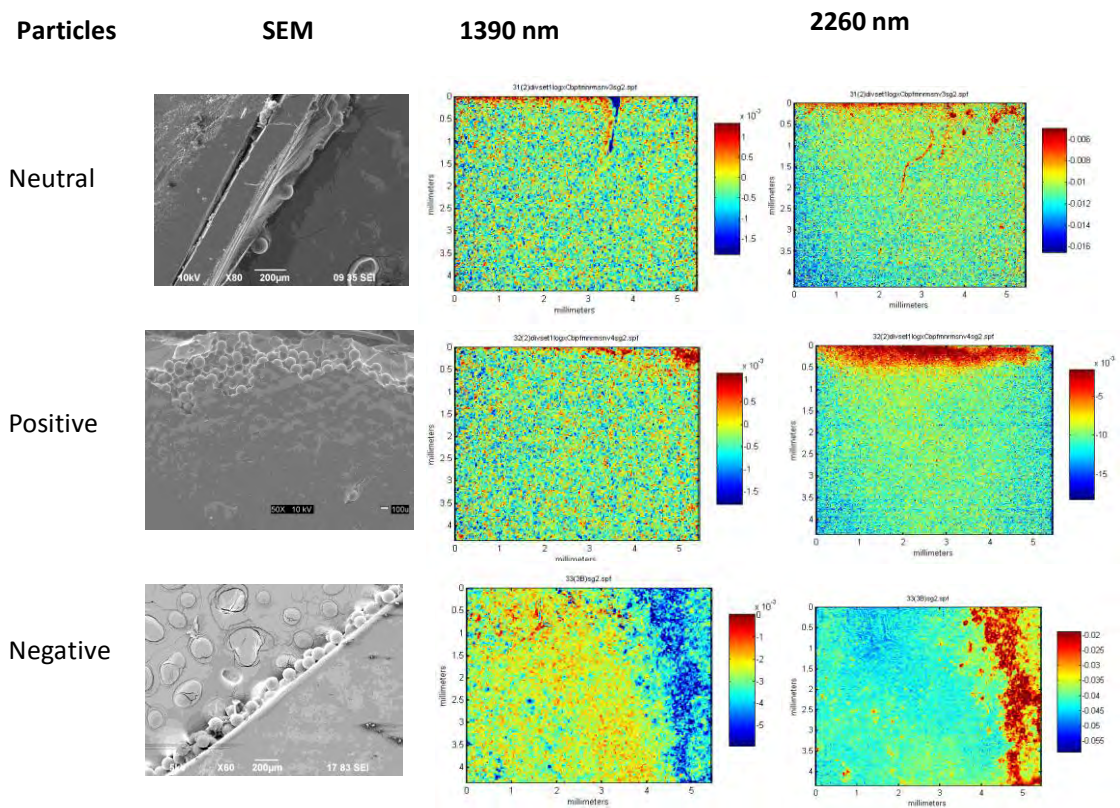


Figure 6. 14NIR chemical image and SEM images for negative membrane with 100 µm silica particles with low (2.2 w/w%) concentration composed of different charges.

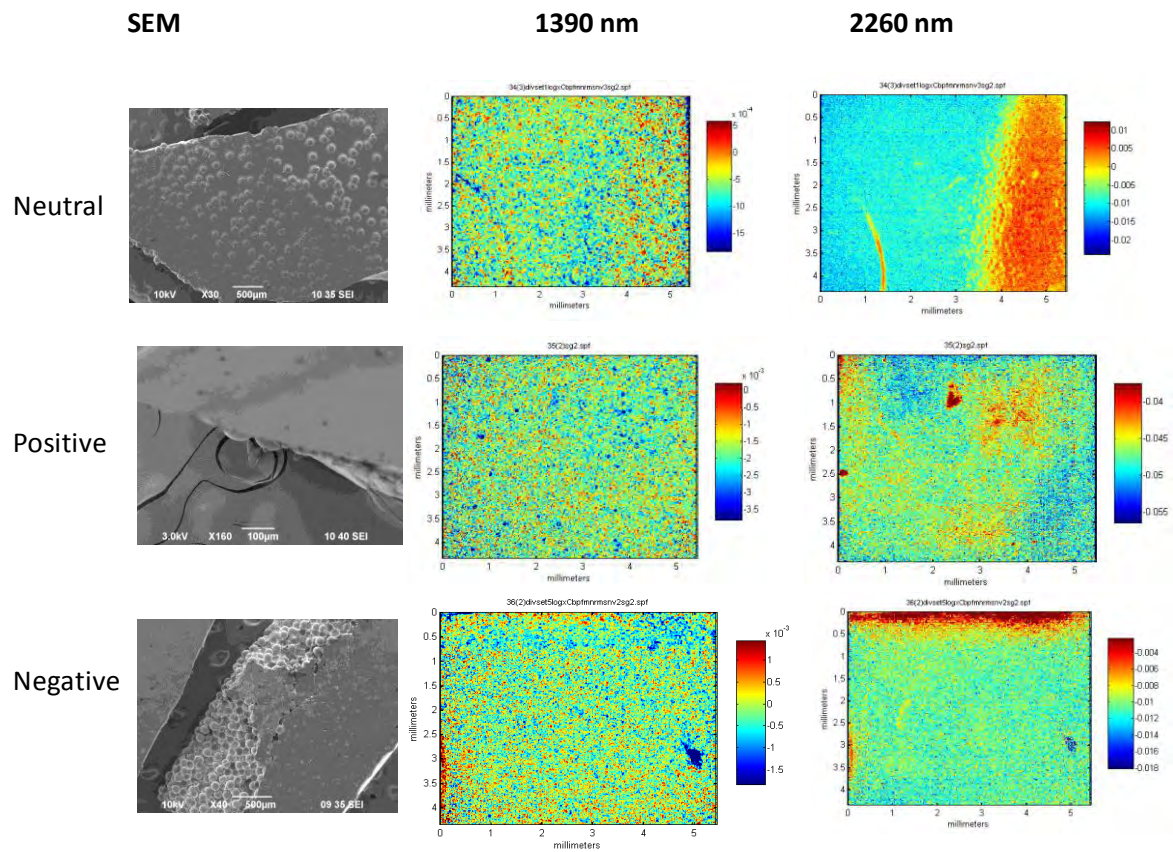


Figure 6. 15 NIR Chemical image and SEM for negative membrane with 100 µm silica particles and high concentration (4.4 w/w%) with different charges.

Research tried to simulate via Monte Carlos the work of Ise et al, the interaction between same charge particles. Feng et al compared the amount of particles, the number of charge per particles and the electrolytic concentration in the solution. This research concluded that large charge per particles and particle volume fractions produce extraordinarily ordered arrangement, while smaller charge per particles and particle volume fractions produce aggregation. Literature accredited this phenomenon to Coulomb interaction between all the charged species. The van der Walls interactions are insignificant and only that can be presents are the electrostatics [13]. The aggregation present in the hydrogels can be caused by this phenomenon. Particle concentration inside the membrane probably is not high enough to make the particles repel, therefore they attract generating big clusters as was observed in the chemical imaging of positive and negative hydrogels.

Other important information that can be obtain in the qualitative study is that positive, neutral and negative membranes analysis with NIR and SEM proved that the particles were encapsulated inside each hydrogel, the NIR technique was able to observe where the particles are located and the SEM area was not enough to conclude about clusters. When NIR and SEM are compared NIR is a better technique because it is able to see larger areas than SEM and explain the chemistry of the sample. NIR and SEM studies were done with 1 μm and 100 nm particles, it is explained in the next section.

6.4.2.2 NIR quantitative inspection of particle distribution

A qualitative study of particle dispersion was done. It is important to determine the quantitative distribution of silica particles in the different hydrogels and compare these results with those obtained qualitatively. For this purpose, chemical images obtained at 2260 nm were converted to a binary image with ISys® software. Figure 6.16 show the conventional image, the chemical imaging and the binary image of a negative membrane with visible silica particles. Figure 6.16 c) presented the binary image which possesses two colors. In this particular case black represents the polymer and white represents the hydrogel, as the conventional imaging where the particles can be easily

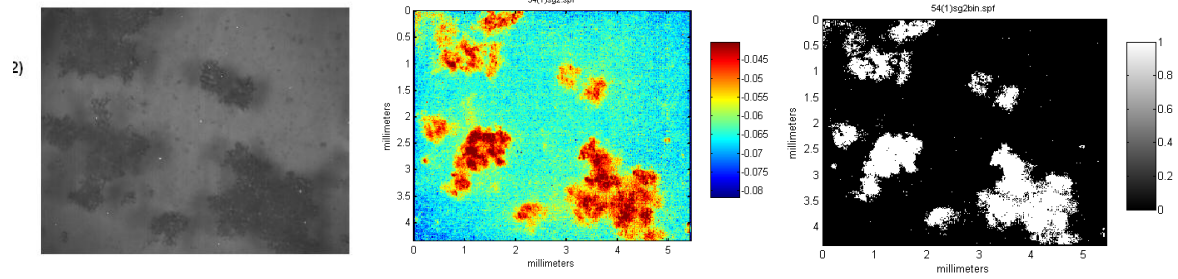


Figure 6. 16 Example of a binary image of DMAEM with silica negative charge particles at 2260 nm. A) Conventional image, b) Chemical imaging, c) Binary image.

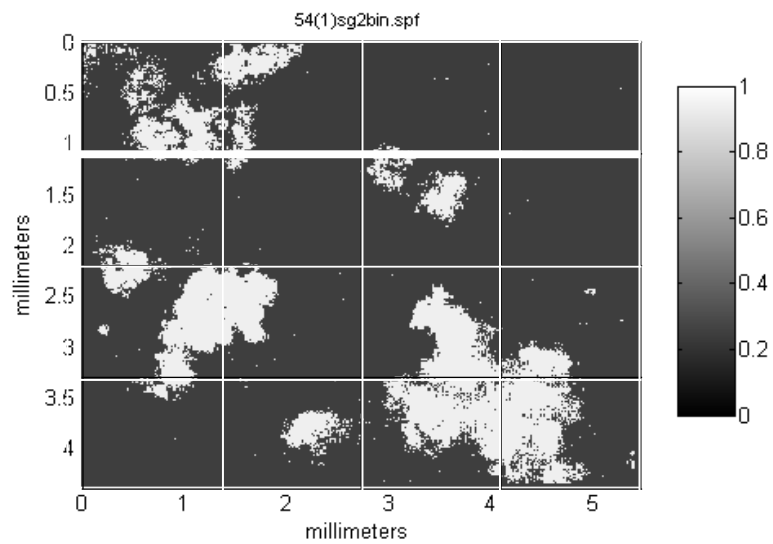


Figure 6. 17 Example of a binary image of DMAEM with silica negative charge particles at 2260 nm with 16 equal squares.

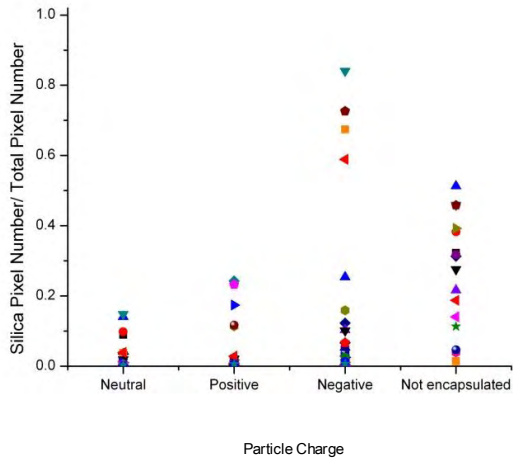
located. The black and white image is the one analyzed in the quantitative inspection. ISys® software produces a binary matrix, according to the binary image, where 1 is silica and 0 is polymer. The binary image was divided into 16 equal squares; see figure 6.17, and the average and standard deviation was calculated as a function of the number of pixels of silica in each area according to equation 6.1

$$R = \frac{\text{Number silica pixels}}{\text{Number Area pixels}} \quad (6.1)$$

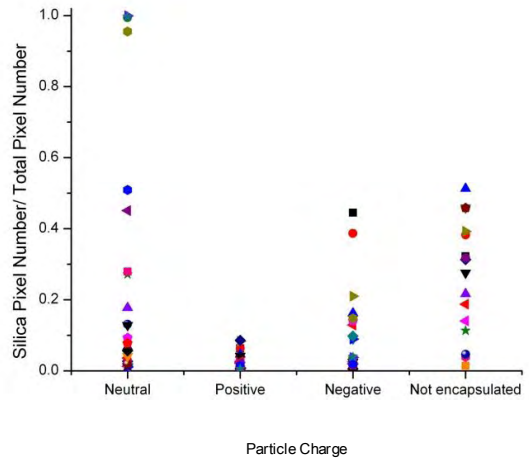
Neutral, positive and negative membranes was quantitative analyzed with 100 µm. Figure 6.18, 6.19 and 6.20 shows each square average for high and low concentration of particles (2.2 w/w% and 4.4 w/w%), and neutral, positive and negative particles of the three scans areas Each point represents the average of silica pixels in a square. Axes X is the particles charge and axes Y is the average where the maximum value is one (1) meaning a membrane area where there is only silica particles and the minimum value is zero (0) meaning a membrane area where there is only polymer. All membranes are compared with a heterogeneous membrane; this membrane was created placing silica particles above the hydrogel already polymerized without particles and dry. The heterogeneity was forced to compare with encapsulated particles.

Figure 6.18 has the silica pixel average distribution for positive membranes. The most homogenous membrane is when negative particles were added at low concentration, because pixel average is similar for all squares. The most heterogeneous distribution is when negative particles were added to the hydrogel, because average values change from 0 to 0.65. The not encapsulated membrane or forced heterogeneous membrane is similar to the hydrogel with negative particles.

Figure 6.19 presented the silica pixel distribution for negative membranes. The most homogenous membrane is when neutral particles were added at high concentration, because pixel average is similar for all squares, between 0 and 0.10. The

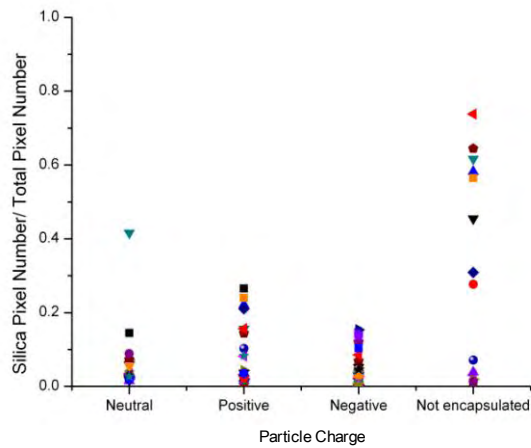


a) Low particles concentration

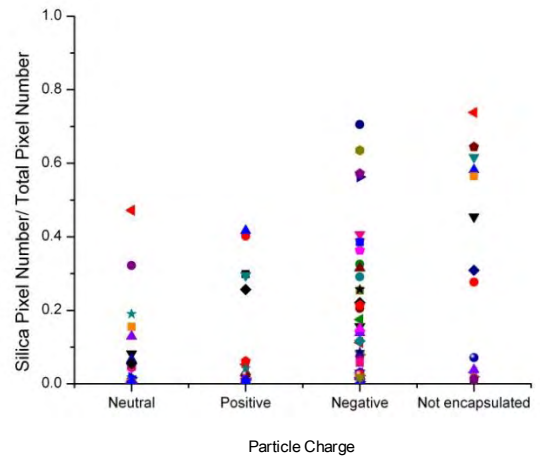


b) High particles concentration

Figure 6. 18 Average R particle distributions in positive hydrogels with 100 μm , different particle charge and two particle concentration.



a) Low particles concentration



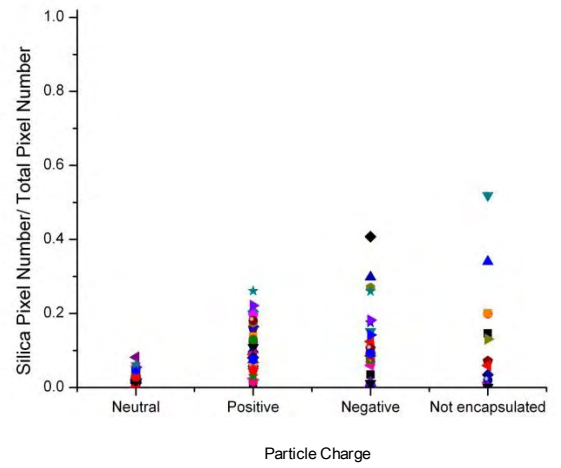
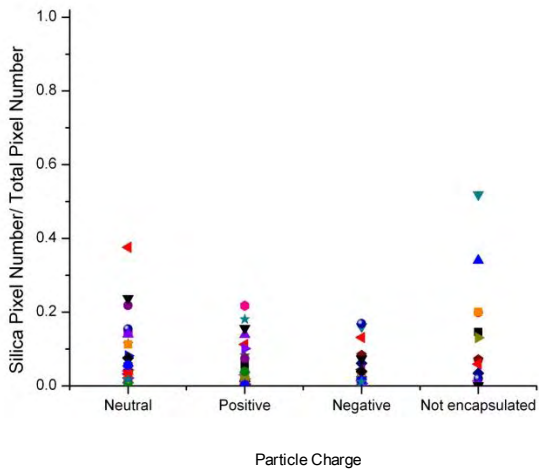
b) High particles concentration

Figure 6. 19 Average R particle distributions in negative hydrogels with 100 μm , different particle charge and two particle concentrations

most heterogeneous distribution is when negative particles at high concentration were added to the hydrogel, because average values change from 0 to 1. The heterogeneous forced membrane has different average values from 0 to 0.5.

Figure 6.20 presented the silica pixel distribution for neutral membranes. The most homogenous membrane is when neutral particles were added at high concentration, because pixel average is similar for all squares, between 0 and 0.10. The most heterogeneous distribution is when negative particles at high concentration and neutral particles at low concentration were added to the hydrogel, because average values change from 0 to 0.40. For neutral membranes the average of the heterogeneous forced hydrogel goes from 0 to 0.55, highest values than encapsulated membranes.

When figures 6.18, 6.19 and 6.20 are compared is observed that neutral membrane has the lower average per membrane and positive and negative membranes has bigger variation between average, therefore neutral membranes has a more homogenous particles distribution and positive and negative membranes has a heterogeneous particles distribution. Qualitative analysis also concluded that the neutral membranes had a homogenous distribution and positive and negative membranes a heterogeneous distribution. Quantitative analysis helps to ratify the visual observation of the chemical imaging.



a) High particles concentration

b) Low particles concentration

Figure 6.20 Average R particle distributions in neutral hydrogels with 100 μm , different particle charge and two particle concentrations

A statistical hypotheses test was done to compare the particles concentration set in the pre-polymeric solution (2.2 w/w% and 4.4 w/w%) and the obtained in the hydrogel in each binary square in the quantitative inspection. Test of hypotheses on the mean of a normal distribution, variance unknown was used for the analysis [14]. For low concentration each R of equation 6.1 was compared with 2.2 w/w % and for high concentration was compared with 4.4 w/w%. The null hypothesis is $H_0: \mu = 2,2$ for low concentration and $\mu = 4,4$ for high concentration, $H_1: \mu \neq 2,2$ for low concentration and $\mu \neq 4,4$ for high concentration. Appendix II presents a calculus model. Table 6.4 presents the H_0 percent rejected by the hypothesis at the 0.05 level of significance. The percent where the hypothesis is not accomplished is higher than 60%, this means that the proposed particles concentration was not achieved in the hydrogel due to the chemical interaction between particles and membranes. Even the neutral hydrogel that presented a most homogenous configuration the concentration in each square is not statistically the same as the added to the hydrogel, especially for high concentration. When low concentration is added a more homogeneous distribution was achieved, because more averages were equal to the initial values, the low concentration percent values are higher than high concentration percent values.

Table 6.4 Rejected Percent of the null hypothesis for low and high particles concentration.

Membrane	Particles	Low Concentration (2.2 w/w%)	High Concentration (4.4w/w%)
Positive	Neutral	25 %	81.25 %
	Positive	43.75 %	77.08%
	Negative	62.5%	96.99%
Neutral	Neutral	64.58%	66.67%
	Positive	71.87%	75%
	Negative	62.5%	81.25%
Negative	Neutral	68.75%	84.38
	Positive	70.83%	75%
	Negative	75%	90.63%

6.4.2.3 1 μm and 100 nm Particle Encapsulation in hydrogels

The comparison the particles distribution using different particles size is one investigation objective. Three different diameters were chosen 100 μm , 1 μm and 100 nm. Smaller particles of 1 μm were analyzed using the same aforementioned analysis. These particles were two orders of magnitude smaller than the previous. Therefore, care must be taken as to how the aforementioned procedures can or cannot determine the presence of clusters if any.

NIR and SEM were also used to study the 1 μm particles distribution inside the hydrogels. Figure 6.21, 6.22 and 6.23 present chemical images at 2260 nm and SEM pictures from 1 μm particle encapsulation in positive, negative and neutral hydrogels at low concentration (2.2 w/w%) and high concentration (4.4 w/w%). Negative membranes SEM images, figure 6.21, do not have clusters, for both concentration, but NIR figures report some clusters for high particles concentration. Positive membranes SEM images, figure 6.22, do not present high particles aggregation and NIR images look very homogeneous, big cluster are observed only with neutral particles at low concentration and positive particles at high concentration. Neutral membranes SEM images, figure 6.23, show big clusters for neutral particles at low and high concentration and NIR images also report clusters for the same membranes.

When the particle size is reduced from 100 μm to 1 μm is necessary to evaluate the NIR capability. NIR objective used was 17.5 μm creating a pixel of 17.5 x 17.5 μm , the particle diameter is 1 μm , and therefore to observe particles is necessary cluster of at least 17.5 μm diameters. The cluster observed in figure 6.22, 6.23 and 6.24 are agglomeration with diameters large than 17.5 μm . Particle size is the limitation of NIR. In this section the homogeneity definition depend on what the NIR is able to see and cluster size according to the objective used. So, all red areas in the chemical imaging are agglomeration of figures 6.21, 6.22 and 6.3.

The quantitative studies were also performed with the 1 μm particles. Figures 6.24, 6.25 and 6.26 for negative, positive and neutral hydrogels for low and high concentration, 2.2 w/w% and 4.4 w/w% present the silica pixel average for each charged particle. The clusters size detected by the NIR is constant over the membrane for almost all combination of particles because the silica pixel average goes from 0 to 0.1. The clusters created are really small and the relation silica pixel: total pixel is low too. The NIR cannot explain which the real particle distribution inside the hydrogel is.

A statistical hypotheses test was also done to compare the 1 μm particles concentration set in the pre-polymeric solution (2.2 w/w% and 4.4 w/w%) and the obtained in the hydrogel in each binary square in the quantitative inspection. Test of hypotheses on the mean of a normal distribution, variance unknown was used for the analysis [14]. For low concentration each R of equation 6.1 was compared with 2.2 w/w % and for high concentration was compared with 4.4 w/w%. The null hypothesis is $H_0: \mu = 2,2$ for low concentration and $\mu = 4,4$ for high concentration, $H_1: \mu \neq 2,2$ for low concentration and $\mu \neq 4,4$ for high concentration. Table 6.5 presents the H_0 percent rejected by the hypothesis at the 0.05 level of significance. The percent varies from 0 to 59% indicating really different behaviors. When 0 % is reported this mean that no average was equal to the initial concentration. The observed clusters presented a more homogeneous distribution at low concentrations, because high percent are reported.

Smaller particles were studied too, 100 nm particle diameters, this particle size is not detected by SEM and neither by the NIR., therefore a particles distribution study was not perform. The NIR images of 100nm particles are shown in the Appendix III.

Table 6.5 Rejected Percent of the null hypothesis for low and high particles concentration.

Membrane	Particles	Low Concentration (2.2 w/w%)	High Concentration (4.4w/w%)
Positive	Neutral	28%	15%
	Positive	29%	2%
	Negative	16%	3%
Neutral	Neutral	31%	28%
	Positive	59%	6%
	Negative	10%	28%
Negative	Neutral	17%	0%
	Positive	31%	25%
	Negative	0%	0%

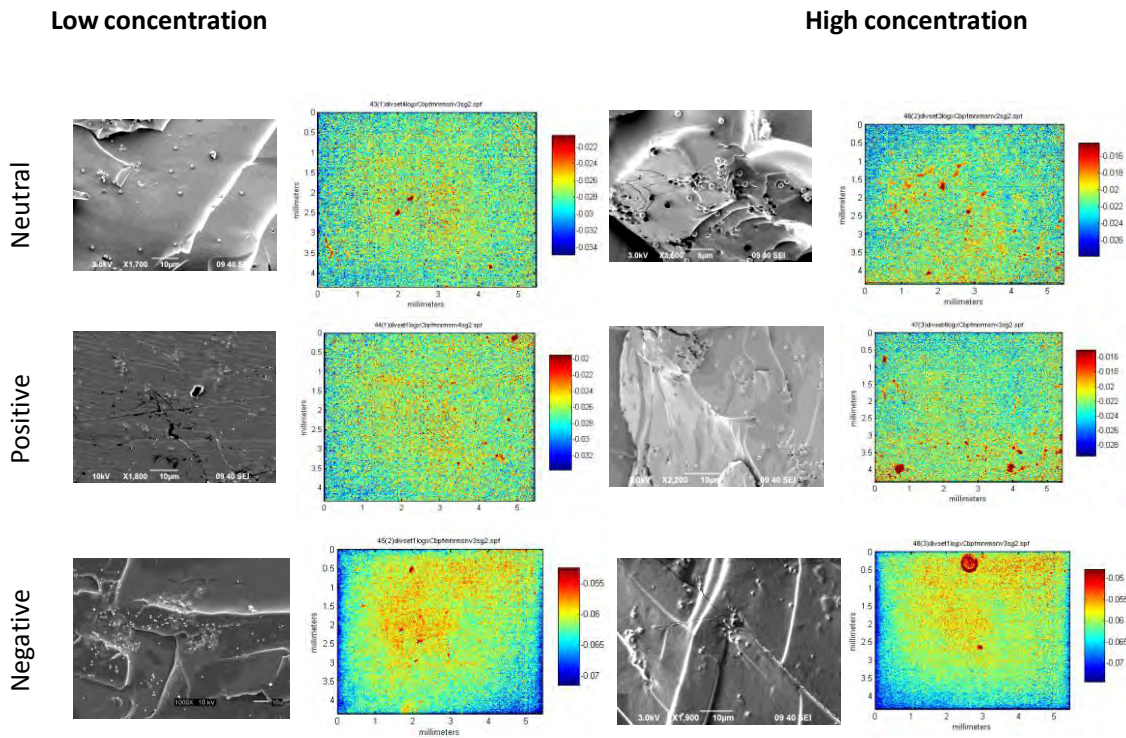


Figure 6.21 Positive membrane with 1 μ m particles and low (2.2 w/w%) and high (4.4 w/w%) concentration SEM and NIR images at 2260 nm.

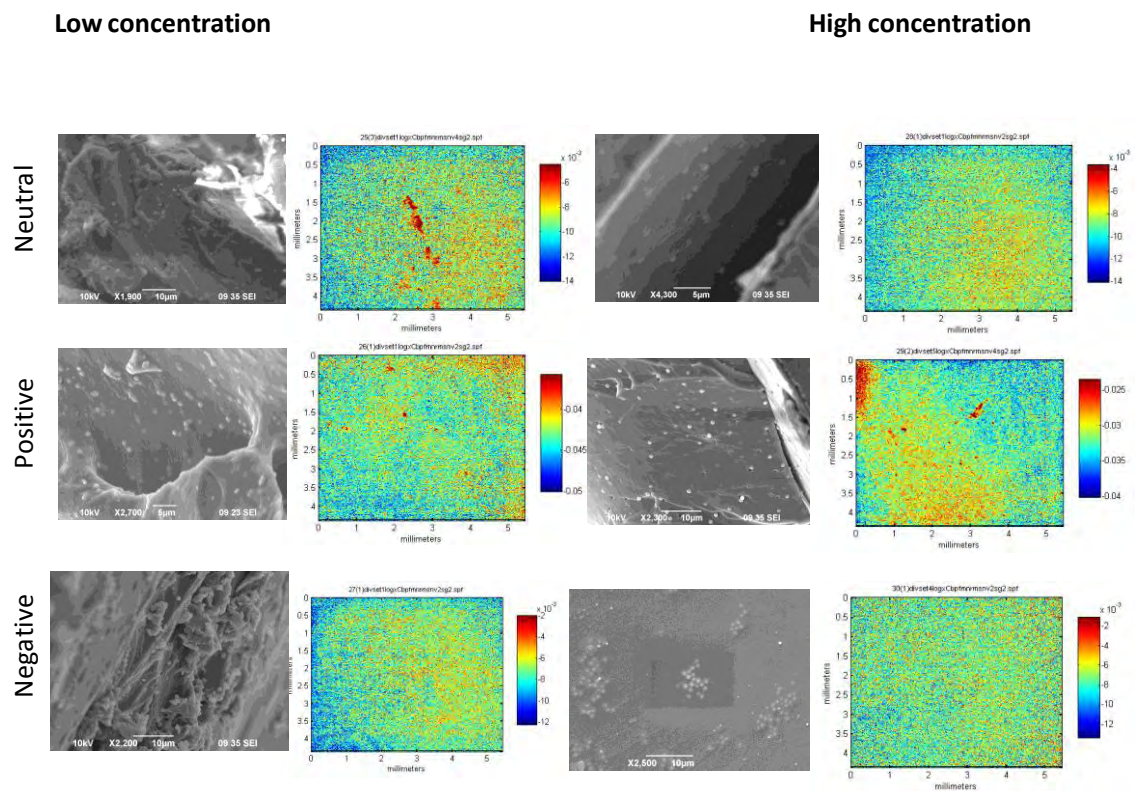


Figure 6.22 Negative membrane with 1µm particles and low (2.2 w/w%) and high (4.4 w/w%) concentration SEM and NIR images at 2260 nm.

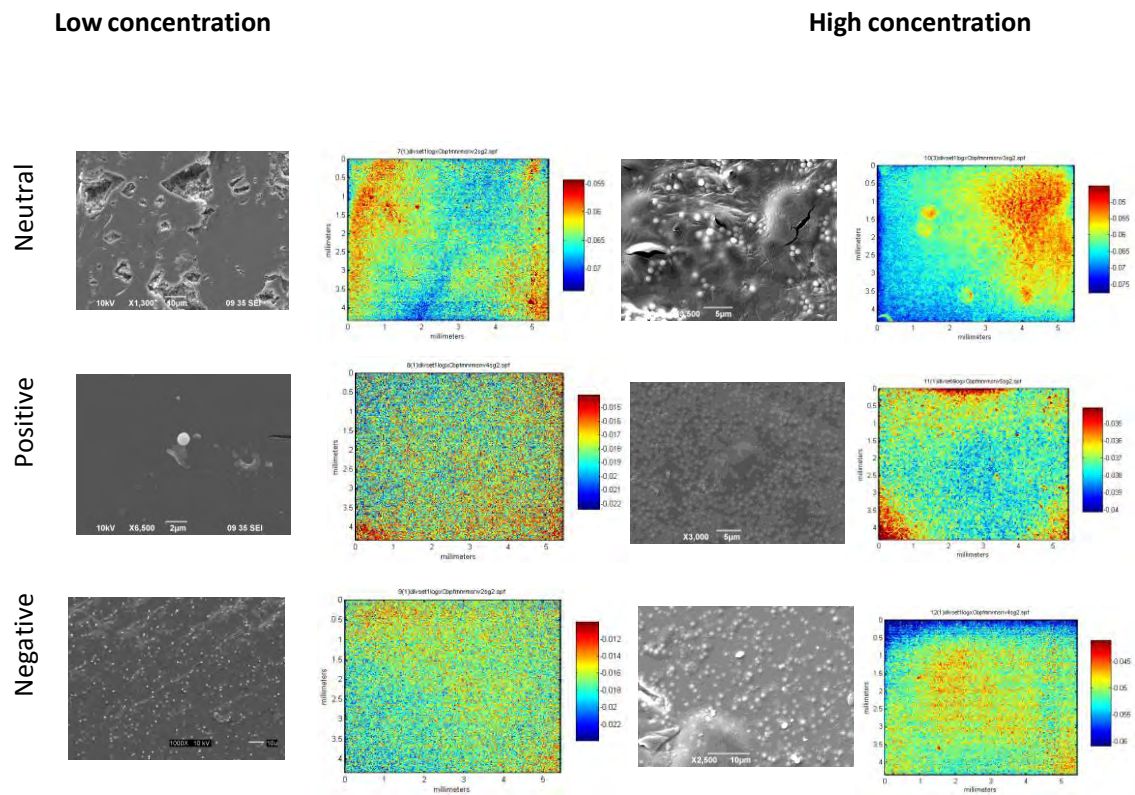
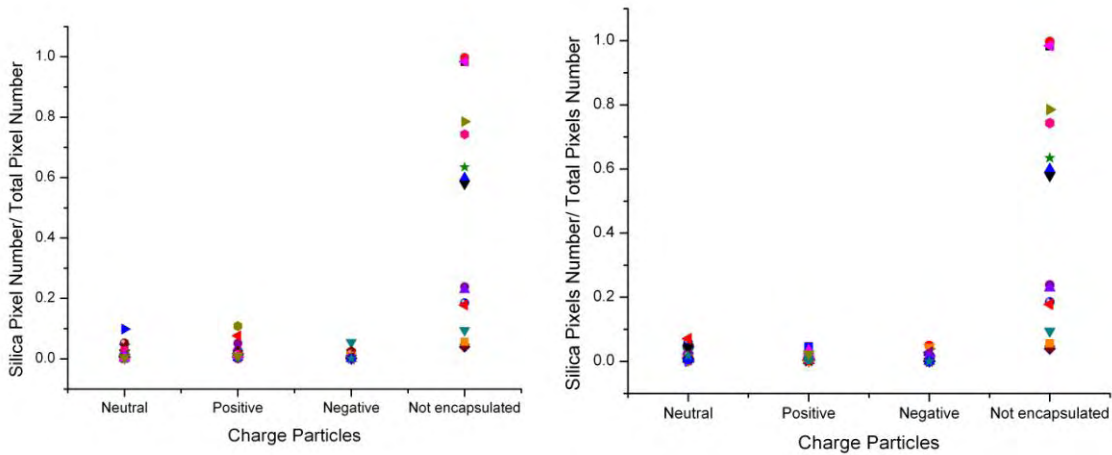


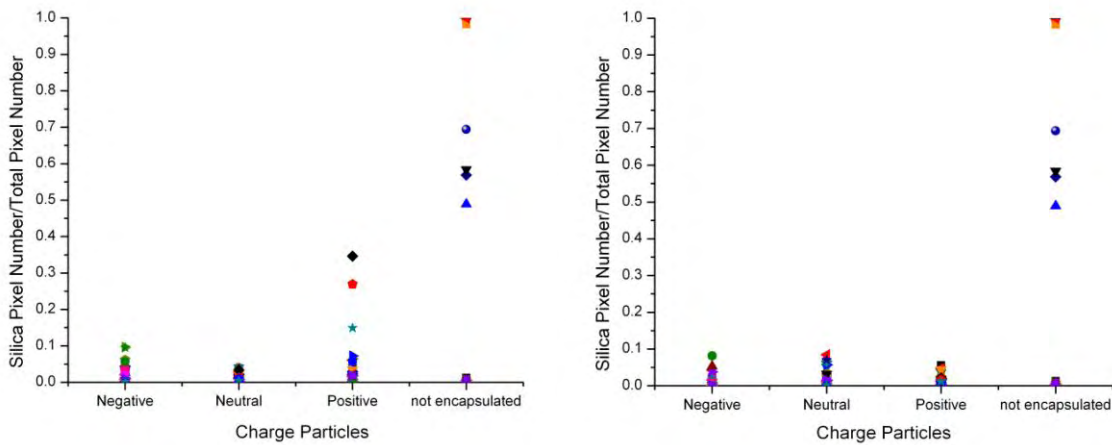
Figure 6.23 Neutral membrane with 1µm particles and low (2.2 w/w%) and high (4.4 w/w%) concentration SEM and NIR images at 2260 nm.



a) Low particles concentration (2.2 w/w%)

b) High particles concentration (4.4 w/w%)

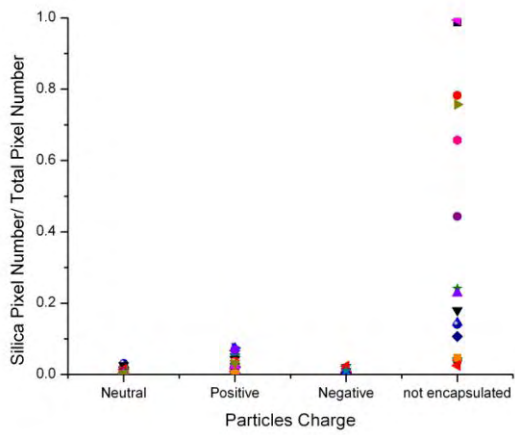
Figure 6. 24 Average R particle distributions in positive hydrogels with 1 μm , different particle charge and two particle concentrations.



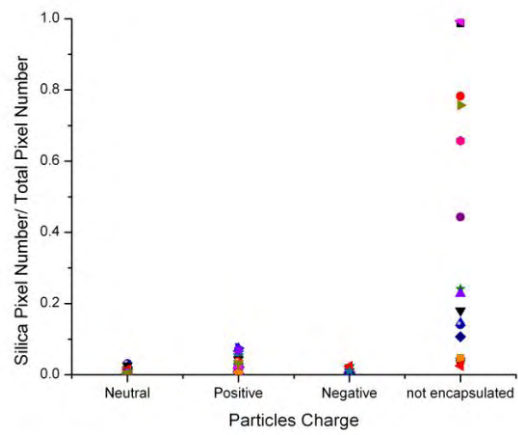
a) Low particles concentration (2.2 w/w%)

b) High particles concentration (4.4 w/w%)

Figure 6. 25 Average R particle distributions in neutral hydrogels with 1 μm , different particle charge and two particle concentration.



a) Low particles concentration (2.2 w/w%)



b) High particles concentration (4.4 w/w%)

Figure 6. 26 Average R particle distributions in negative hydrogels with 1 μm , different particle charge and two particle concentrations.

6.5 Conclusions on particles distribution

First, NIR and SEM are techniques were employed to assess particle distribution. NIR proved, for this particular application, to be a better technique, because a bigger tridimensional area is observed and several chemical structures can be detected. SEM advantage is the ability to observe small particles (1 μm) inside polymers whereas NIR is a technique able to detect particles bigger than 10 μm . Therefore, the intended analysis of this work was only performed with the 100 μm particles, which provided the means to perform both a qualitatively and quantitatively analysis. Qualitative and quantitative analysis concluded that particle distribution in hydrogels do depend on the membrane charge. Ionic membranes generated heterogeneous particle distribution and neutral membranes created a more homogenous particles distribution. In Neutral membranes identical charged particles present electrostatic repulsion between them because there is not any ion or functional group that interacts with the particles and for ionic membranes particles need high charge and high particle volume fractions to produce electrostatic repulsion.

6.6 References

- [1] K. Awa, T. Okumuraa, H. Shinzawa, M. Otsuka and Y. Ozaki. "Self-modeling curve resolution (SMCR) analysis of near-infrared (NIR) imaging data of pharmaceutical tablets." *Analytical Chimica Acta*, 619, pp. 81–86, 2008.
- [2] J. Amigo, J. Cruz, M. Bautista and S. Maspocho, J. Coello and M. Blanco. "Study of pharmaceutical samples by NIR chemical-image and multivariate analysis". *Trends in Analytical Chemistry*, 27, pp. 696-713, 2008.
- [3] A. Gowen, C. O'Donnell, P. Cullen and S. Bell. "Recent applications of Chemical Imaging to pharmaceutical process monitoring and quality control". *European Journal of Pharmaceutics and Biopharmaceutics*, 69, 10–22, (2008).
- [4] S. Sasic. "Chemical imaging of pharmaceutical granules by Raman global illumination and near-infrared mapping platforms". *Analytical Chimica Acta*. 611, pp. 73–79, 2008.
- [5] K. Bakeev, *Process Analytical Technology*, Blackwell Publishing, 2005
- [6] T. Furukawa, H. Sato, H. Shinzawa, I. Noda and S. Ochiai. "Evaluation of Homogeneity of Binary Blends of Poly(3hydroxybutyrate) and Poly(L-lactic acid) Studied by Near Infrared Chemical Imaging (NIRCI)" *Analytical Sciences*, 23, pp.871-876, 2007.
- [7] K. L. A. Chan, N. Elkhider and S. G. Kazarian, "Spectroscopic Imaging Of Compacted Pharmaceutical Tablets" *Chemical Engineering Research and Design*, 83, pp. 1303–1310, 2005.
- [8] L.Hilden, C. Pommier, S. Badawy and E. Friedman. "NIR chemical imaging to guide/support BMS-561389 tablet formulation development" *International Journal of Pharmaceutics*, 353, pp. 283–290, 2008.
- [9] Instruction Manual for Using the BI_ZTU The Autotitrator for Use with Brookhaven's Zeta Potencial Instrument., Brookhaven Instrument Corporation, 2005.
- [10] G. D. Chukin and V. I. Malevich, "Infrared Spectra of Silica" *Journal of Applied Spectroscopy*, 26, pp. 294–301, 1977.
- [11] L. G. Webber and S. C.Lo *Spectra–Structure Correlations in the Near-infrared*", John Wiley & Sons Ltd, 2002.
- [12] A. M. Efimov and V. G. Pogareva "IR absorption spectra of vitreous silica and silicate glasses: The nature of bands in the 1300 to 5000 cm⁻¹ region", *Chemical Geology*, 229, pp. 198–217, 2006.

[13] J. Feng and E. Ruckenstein, "Attractive interactions in dispersions of identical charged colloidal particles: a Monte Carlo simulation" *Journal of Colloid and Interface Science*, 272,pp. 430–437, 2004.

[14] D. Montgomery and G. Runger, *Applied Statistics and Probability for Engineers*, Wiley, 1994.

7 Effect of Encapsulated Particles on the Mechanical Properties of Crosslinked Hydrogels.

7.1 Introduction

Rheology provides the means to describe polymer dynamics by studying fluid flow and deformation [1]. Rheology can be classified into steady, dynamic and transient flows [1]. In this investigation dynamic shear rheology was investigated in hydrogels membranes containing silica particles to determine the effects of particle charge, charge and the various membrane compositions, on the storage and loss modulus of the resulting composites. Rheological measurements can be used to get an insight in the product structure in relation between viscosity of a suspension and the size, number and shape of the suspended particles [2].

Dynamic shear rheology measures the resistance to dynamic oscillation flows, steady shear viscosity is a measure of resistance to steady shearing deformation and transient shear flows involve examining the shear stress and viscosity response to a time dependent shear. Dynamic shear analysis is the simplest method to give structural information about the sample. Dynamic modulus also had been used to investigate the pseudo solid-like behavior of polymers and the formation of a three dimensional network [3].

Hydrogels are composed of chemical crosslinkers and reactive monomers. The science that studies the deformation of properties of reactive polymers is named chemorheology [1]. For the chemorheology, it is important to understand that these chemically crosslinked hydrogels present several steps until its final three dimensional network is formed. First, the unreacted monomers start to form branched molecules, then the reaction continues until the gel point is reached and an infinite network is formed across the whole structure [1]. The gel point is the transition from liquid-like behavior to solid-like behavior [3].

In this investigation viscoelastic behavior is the one analyzed when particles are added to the network formation. The dynamic properties or the dynamic shear rheology is measured with the resistance to dynamic oscillatory flows [1]. The important variables

are the storage modulus (G') and the loss modulus (G''). They are employed to characterize the deformation resistance to a dynamic oscillation [1]. The storage modulus refers to the storage of elastic energy and the loss modulus characterizes the viscous dissipation of that energy. The loss tangent is high for materials that are liquid-like, but is low for materials that are solid-like [4].

The dynamic properties can explain if the gel has a linear viscoelastic behavior, but it is reported that reactive systems generally do not present this type of behavior. These systems are characterized by dynamic properties that diverge at different strain amplitude and to be linear they must be independent of the strain amplitude [1]. Then the polymer viscoelastic behavior needs to be analyzed as a function of temperature and reaction time to fully achieve the description of it [1].

In this chapter the dynamic shear behavior of crosslinked hydrogels is described when particles are added during the reaction. It is necessary to understand the change in the viscoelasticity when the gel and particle charge is modified, because literature report an improvement in mechanical properties when inorganic exfoliated clay minerals are added to polymeric matrices [9].

7.2 Literature Review

When polymers are crosslinked their properties change from a viscous liquid to an elastic solid. Liquid viscosity deviates to infinity at the gel point and the low frequency modulus increases from zero [4]. Rheology can help describe the mechanical behavior of hydrogel with embedded particles. Some previous work has described different factors involved in the effect of particles in the mechanical properties of a matrix.

Dynamic properties and reaction kinetics for hydrogels have been studied predominantly analyzing the concentration of crosslinker in the sample. Lin-Gibson and colleges worked with chitosan and water soluble blocked diisocyanate crosslinker and studied the reaction kinetics and the gel modulus, loss and storage. The gelation time was determined through two different methods, rate equivalence of the change in modulus as a function of reaction time ($G'G''$ crossover) and the critical gel via the

Winter–Chambon (the point where loss tangent ($\tan \delta$) curves converge when is plotted at different frequencies as function of time), 24 min and 21 min, respectively. The difference in the time value is due to the imposed strain and frequencies employed in the experiments. The effect crosslinker concentration was also studied. Crosslinker concentration was increased from 0 to 50 by mass fraction. The storage modulus increases with the crosslinker concentration because highly crosslinked networks were formed [5].

Sahiner and colleges investigated the rheological behavior of a novel cationic hydrogel, (3-acrylamidopropyl)-trimethylammonium chloride (APTMAC1), crosslinked with a neutral crosslinker (N,N'-methylenebisacrylamide). The elastic modulus or loss modulus near the gel point presented power law dependence. After the gel formation the elastic modulus had exponential dependence on the relation crosslinker/monomer. This work concluded that there is a critical ratio of crosslinker/monomer to form a really isotropic network [3].

Hydrogels have been analyzed in the literature, but it is also important to understand how particles affect the rheology of polymers. Research presented a lot of information about how particles modify the dynamic properties when are added to the polymer.

Katsikis et al investigated the thermal stability of poly(methyl methacrylate) (PMMA) when silica particles are added at elevated temperatures in the molten state. For this purpose, rheological tests were performed and the particle diameter was from 10-120, 250 and 1200 nm. The rheology experiments showed that PMMA storage modulus decrease with time and high temperatures. The composite PMMA with silica resulted in an increase in the storage modulus with time at temperatures of 200°C and over. It was found that the PMMA grafted into the silica. A chemical reaction between the PMMA and the silanol groups was not found [6].

Hu et al compared the storage and loss modulus when poly(lactic-co-glycolic acid) (PLGA) particles were grafted with double carbon bonds containing Gelatin-g-MA (GM) and added to crosslinkable chitosan derivative (CML) hydrogel [6]. The PLGA particles had a diameter of 820 ± 121 nm. The storage modulus improved with the increase of the GM particles. With the same concentration of particles in the hydrogel

and GM particles, gelatin modified particles and blank particles; the one with highest storage modulus was the one with GM particles. This increase is associated with the energy dissipation mechanism. The CML chains are deformed when the force is applied, the energy is dissipated to the particles. When more particles are added stronger energy dissipation is made by the hydrogel and finally a large storage modulus is reported. The GM particles presented a large interfacial action and dissipate the energy more efficiently creating large number of storage modulus. The viscosity is determined by the continuous phase that is the hydrogel, therefore the loss modulus did not change, the particles concentration was really small 0.4% v/v [7].

Particle distribution studies with dynamic properties, from Mitsumata et al. worked on the nonlinear viscoelastic response and relative storage modulus of a composite soft material using poly(vinyl alcohol) composite gel with aluminum hydroxide particles. The dynamic viscoelasticity at volume fractions $\phi < 0.04$ presented random dispersion of particles. The storage modulus did not demonstrate nonlinear viscoelastic response at $\phi < 0.04$. The nonlinear viscoelastic response was recognized at $\phi > 0.06$, suggesting a partial contact between particles and a heterogeneous distribution of particles [8].

Mitsumata et al. also reported the effect of magnetic particles on the significant reduction in the dynamic modulus of carrageenan gels containing barium ferrite and iron oxide particles. The gels containing barium ferrite demonstrated a significant reduction in the storage modulus on the order of 10^5 Pa. The principal cause is the magnetization of the particles, for gels with iron oxide the reduction was less than 10^4 Pa. The storage modulus of gels with barium ferrite above volume fraction of 0.06 shows the heterogeneous dispersion of the magnetic particles and the storage modulus with iron oxide suggested the random dispersion of the particles. Gels with iron oxide exhibited weak nonlinear viscoelasticity and gels with barium ferrite demonstrated enhanced nonlinear viscoelasticity. This is due to the aggregation of the barium ferrite particles that are connected with each other and create a local particle network in the polymer [9].

Kinetic studies for hydrogels without particles and studied the dynamic properties when the concentration of the crosslinker. Literature explained that when particles are added to the polymer the storage modulus increased. Finally, some research has tried to explain particle distribution with rheological dynamic properties. Research in dynamic

rheology had not analyzed systems where the particles charge and the membrane charge is considered [4, 5, 6, 7]. This investigation pretends to understand how the particle charge, size, and membrane composition alter the dynamic properties of hydrogels. The reaction kinetic of the hydrogel also is studied in order to comprehend how the present of particles modify the velocity of the chemical reaction.

7.3 Materials and Methods

The hydrogels for the rheological characterization were prepared by free radical polymerization but the initiator was activated by heat in the rheometer. The same monomers were: methacrylic acid (MAA) monomer, cationic, (N,N-dimethyl amino) ethyl methacrylate (DMAEM) monomer, and neutral: 2-hydroxyethyl methacrylate (HEMA) monomer. The crosslinker poly(ethylene glycol) dimethacrylate (PEGDMA 1000) (n=1000) (PolySciences Inc. Warrington, PA).. See Table 6.1 for hydrogels composition. A solution 1:1 v/v deionized water/ethanol (Fisher Scientific, Pittsburgh, PA) is the diluents. The particles were from silica: plain, aminated and carboxylated with 100 μm diameter from (Corpuscular, Cold Spring, NY). The heat initiator 2,2'-azobisisobutyronitrile (Sigma-Aldrich, St Louis, MO). Hydrochloric acid 6N and sodium hydroxide 1M and 5 M was used to change the pH of the pre-polymeric solution.

The monomer, crosslinker and diluents were weighted in an amber bottle with septum screw caps. The particles were added after the pre-polymeric solution was sonicated and a homogenous mixture was observed. The initiator was added and the mixture was again sonicated and placed in the inert glove box from Cole-Parmer Instrument Co. (Vernon Hills IL) and was bubble with argon for 15 minutes.

Rheological characterization was performed on a Reologica StressTech HR stress-controlled rheometer equipped with an extended temperature cell (ETC) for temperature control using disposable aluminum plate-and-plate (d = 30 mm) in an oscillation strain control test. The rheometer fixture was pre-heated to 60°C, before transferring and loading the solution. A custom made solvent trap was used to prevent evaporation of the solvent. The shear stress modulus (G') and the loss modulus (G'') were measured at a frequency of 1.0, and a strain of 1.00×10^{-2} and 300 measures were taken.

7.4 Results

When particles are added to a polymer its chemical and physical characteristics are modified. The literature does not report a study in how rheological properties change when charged particles and charged polymers are created. Functionalized silica particles were encapsulated in three different charged hydrogels in the rheometer in order to understand the dynamic properties of gels.

The pre-polymeric solution was placed in the plate and plate configuration at 60 °C and was polymerized until the storage modulus reached the stationary state. Figure 7.1 presents the storage modulus over time and how at x seconds the hydrogel reach the stationary state. First, it was necessary to determine if the particles concentration was high enough to change the dynamic properties of the hydrogels. The storage modulus (G') and the loss modulus (G'') were measured for each hydrogel with the non-functionalized particles and 4.4 w/w% particle concentrations at constant temperature. Three measurements were done of each hydrogel and an average was calculated. Table 7.1 present the storage modulus for hydrogels with particles and without particles. The particles concentration is not high enough to make changes in the storage modulus and this was proved with a hypothesis test. The null hypothesis cannot be rejected. For neutral membrane $t_0 = -0.3630$, for positive membrane $t_0 = 2.2280$ and negative membrane $t_0 = -0.1666$. Being $t = 6.314$ for a 0.05 level of significance, meaning average statistically equals. See Appendix II.

The particles charge was modified to observe the storage modulus see table 7.2. Table 7.2 also suggests that the particles concentration used was not enough to observe the charge influence in the dynamic properties and it is not possible to conclude about the dynamic properties.

The particles concentration was increased to observe how the storage modulus changes. Table 7.3 presents the storage modulus for three silica particles concentration in DMAEM hydrogels. The results suggest that the storage modulus increase when the particles concentration increase. The particles probably made the polymer more elastic due the interaction between the particles and the polymer, because the polymer has a

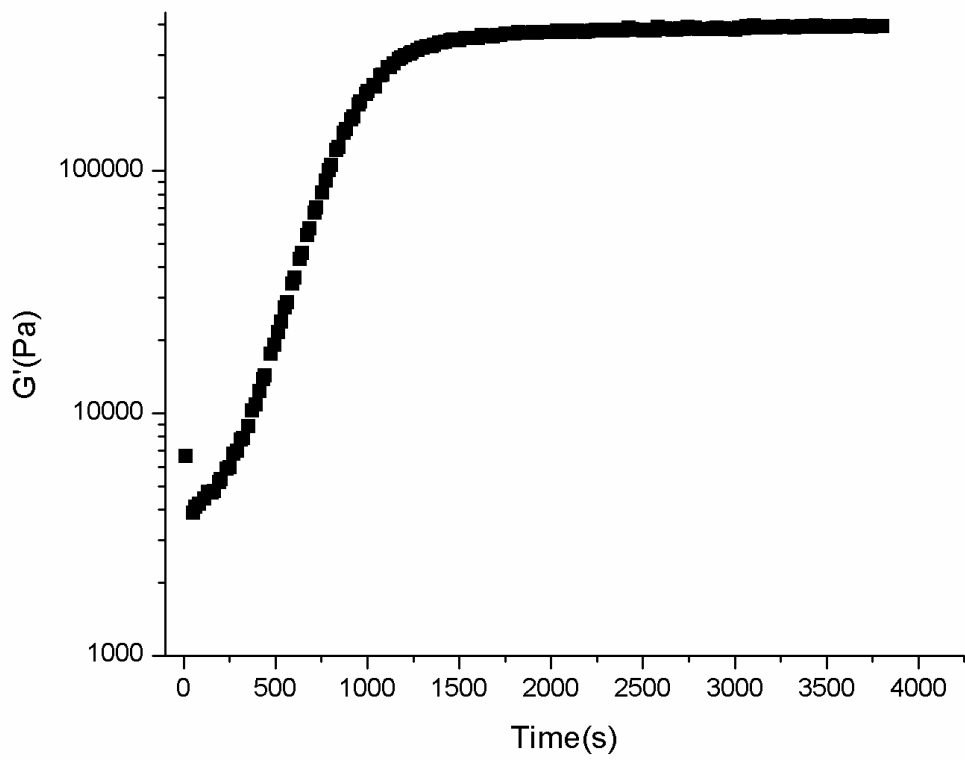


Figure 7.1 Storage modulus in function of time of HEMA hydrogel with 100 μm 4.4 w/w% negative particles

positive charge and particles negative, this made a strong adhesion between them and made more difficult to break.

Fu report that important improvement in mechanical properties of polymers can be achieved by adding inorganic exfoliated clay minerals. Polymer stiffness depends significantly on particles loading because particles have higher modulus than the matrix [10]. Literature conclude that particles loading, size and particle/matrix adhesion affect the strength, stiffness and toughness of particles composite and this three factors created different trends due to the interplay between them [10]. So, it is important to increase the particle concentration to be able to observe how the particles charge influence the storage and loss modulus of hydrogels.

Table 7.1 Storage modulus for different charge hydrogel with encapsulated silica particles of 100 um and 4.4w/w% particles concentration.

G'(Pa)	DMAEM	STD	MAA	STD	HEMA	STD
Polymer without particles	3.66E+05	1.71E+05	3.84E+05	7.44E+04	1.67E+05	1.91E+04
Polymer with silica particles	1.34E+05	4.55E+04	4.04E+05	1.90E+05	1.82E+05	6.63E+04

Table 7.2 Storage modulus for different charge particles in different charge hydrogel of 100 um 4.4w/w% particles concentration

G'(Pa)	DMAEM	STD	MAA	STD	HEMA	STD
Polymer without particles	3.66E+05	1.71E+05	3.84E+05	7.44E+04	1.67E+05	1.91E+04
Negative charge particles	1.34E+05	4.55E+04	4.68E+05		3.88E+05	
Positive charge particles	2.85E+05		4.04E+05	1.90E+05	3.85E+05	
Neutral charge particles	4.58E+05		3.88E+05		1.82E+05	6.63E+04

Table 7.3 Storage modulus for different silica particles with negative charge concentration in DMAEM (positive) hydrogel of 100 um

Particles Concentration	G'(Pa)
4.4 w/w%	1.34E+05
12 w/w%	4.94E+05
16 w/w%	4.59E+05

7.5 Conclusion and recommendations

Particles added to polymers change the dynamic rheology properties of the polymers, according to research, the matrix properties depend on the particles loading, size and particle matrix adhesion. The results suggest an increase in the storage modulus when the particles concentration is increased. The silica concentration must be increased until observe the influence in the dynamic properties when the particle charge and size is changed.

7.6 References

- [1] P. Halley and G. George, *Chemorheology of Polymers*, Cambridge, first edition, 2009.
- [2] Rheology rheometer, Rheology instrument AB, 2000.
- [3] N. Sahiner, M. Singh, D. De Kee, V. John, G. McPherson. "Rheological characterization of a charged cationic hydrogel network across the gelation boundary" *Polymer*, vol. 47, 1124–1131, 2006.
- [4] R. Larson, *The Structure and Rheology of Complex Fluids* Oxford, University Press, 1999.
- [5] S. Lin-Gibson, H. Walls, S. Kennedy and E. Welsh. "Reaction kinetics and gel properties of blocked diisocyanate crosslinked chitosan hydrogels" *Carbohydrate Polymers* 54,193–199, (2003).
- [6] N. Katsikis, F. Zahradnik, A. Helmschrott, H. Münnstedt, A. Vital, "Thermal stability of poly(methyl methacrylate)/silica nano- and microcomposites as investigated by dynamic-mechanical experiments" *Polymer Degradation and Stability*, vol. 92, 1966-1976, 2007.
- [7] X. Hu, J. Zhou, N. Zhang, H. Tan and C. Gao. "Preparation and properties of an injectable scaffold of poly(lactic-co-glycolic acid) microparticles/chitosan hydrogel" *Journal of the Mechanical Behavior of Biomedical Materials*, vol. 1, 35–359, 2008.
- [8] T. Mitsuma, T. Hachiya and K. Nitta. "Nonlinear viscoelasticity, percolation and particles dispersibility of PVA/aluminum hydroxide composite gels". *European Polymer Journal*, vol. 44, pp. 2574-2580, 2008.
- [9] T. Mitsuma, T. Wakabayashi and T. Okazaki, "Particle Dispersibility and Giant Reduction in Dynamic Modulus of Magnetic Gels Containing Barium Ferrite and Iron Oxide Particles". *J. Phys. Chem.*, vol. 112, pp. 14132-14139, 2008.
- [10] S. Fu, X. Feng, B. Lauke and Y. Mai, "Effects of particle size, particle/matrix interface adhesion and particle loading on mechanical properties of particulate–polymer composites, *Composites: Part B*, 39, pp. 933–961, 2008.
- [11] S. Van Tommea, M. Steenbergena, S. De Smedtb, C. van Nostruma, W. Henninka, "Self-gelling hydrogels based on oppositely charged dextran microspheres", *Biomaterials*, 26, pp.2129–2135, 2005.

8 Conclusions

Particle encapsulation in polymer systems has been used in several industrial applications as the film strips, which has been employed for the oral delivery of therapeutic agents. The challenge in particles distribution for pharmaceutical film strips is that the particles must be homogeneously dispersed within the membrane to guarantee equal dosing. For this reason it important to understand the chemical and physical aspects that controls particle distribution. Physicochemical interactions of particles distributed in polymeric membranes had not been fully understood. In this investigation, particle distribution was analyzed as a function of substrate and particle charge, as well as particle size and concentration.

A qualitative and quantitative analysis was done to examine the particles distribution in all synthesize membranes. Results from the qualitative analysis with NIR and 100 μm particles indicated that particle distribution in hydrogels depend on the membrane charge and particle concentration. Ionic membranes created heterogeneous particles distribution due to the low charge and volume fraction present in the membranes. With higher concentration the electrostatic repulsion can create more homogeneous membranes. Neutral membranes create homogenous membranes, because there is not any ion or functional group that interacts with the particles.

The quantitative particles distribution study with the NIR and 100 μm particles concluded that 100 μm particles quantitative analysis proved that neutral membranes had a smaller clusters and similar area average comparing with positive and negative hydrogels. The hypothesis test concluded that with 100 μm particles at low concentration the synthesized membranes presented a more homogenous particles distribution, because the more averages were equal to the initial concentration. The qualitative and quantitative of 1 μm particles with the NIR showed only the clusters with diameters larger or equal than 17.5 μm , so a particles distribution behavior was not observed.

Rheology measurement showed that the particles concentration was small to modify the dynamic properties of the hydrogels without particles. It is recommended to increase the particles concentration to observe how charge and size particles affect storage and loss modulus.

The physicochemical interaction between particles and membranes had not been fully developed in the literature. According to this investigation the membranes charge and the particles concentration are the principal physicochemical factors that control the particles distribution in chemical cross-linker hydrogels. Neutral membranes and low concentration particles created a more homogenous particle distribution. The hydrogels mechanical properties depend on the particles concentration present in polymerization.

APPENDIX I

NIR Chemical image of HEMA and MAA

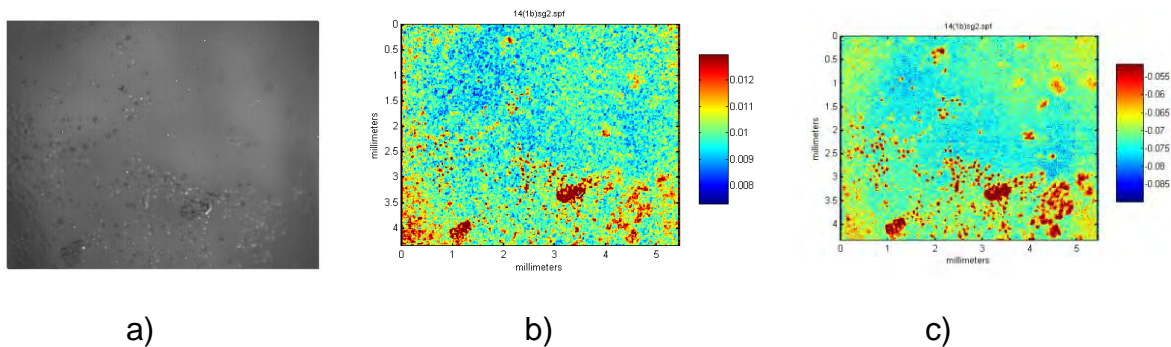


Figure I.1. HEMA with negative 100 μm particles, a) Conventional microscopy image, b) NIR chemical imaging at 1390 nm, c) NIR chemical imaging 2260 nm.

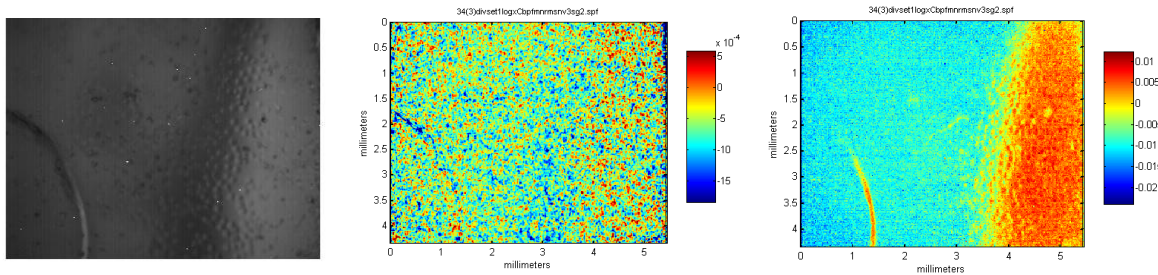


Figure I.2. MAA with negative 100 μm particles, a) Conventional microscopy image, b) NIR chemical imaging at 1390 nm, c) NIR chemical imaging 2260 nm.

APPENDIX II

Calculus model for hypothesis test in quantitative analysis

$$H_0 = \mu = \mu_0$$

$$H_1 = \mu \neq \mu_0$$

If $t_0 > t_{0,05,31}$, then H_0 is rejected

The calculus model for negative membrane with 100 μm positive particles and 4.4 w/w% concentration.

X =Average

μ_0 =parameter of study

s = standard deviation

n =sample number

$$t_0 = \frac{X - \mu_0}{s/\sqrt{n}} = \frac{0.007227 - 0.044}{0.0842/\sqrt{320}} = 7.756$$

$t_0 > t_{0,05,31} = 1.695$, and H_0 is rejected

APPENDIX III

NIR Chemical Images of 100 nm particles encapsulation

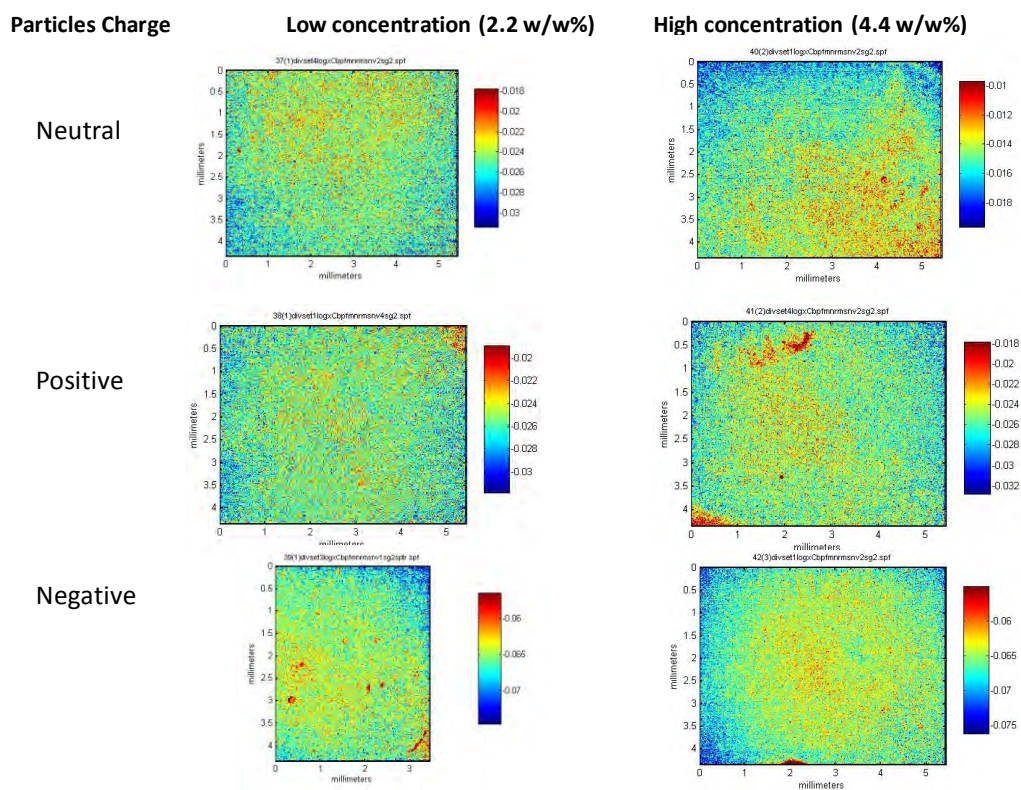


Figure III. 1Chemical imaging of positive membrane with 100 nm particles at high and low concentration at 2260 nm

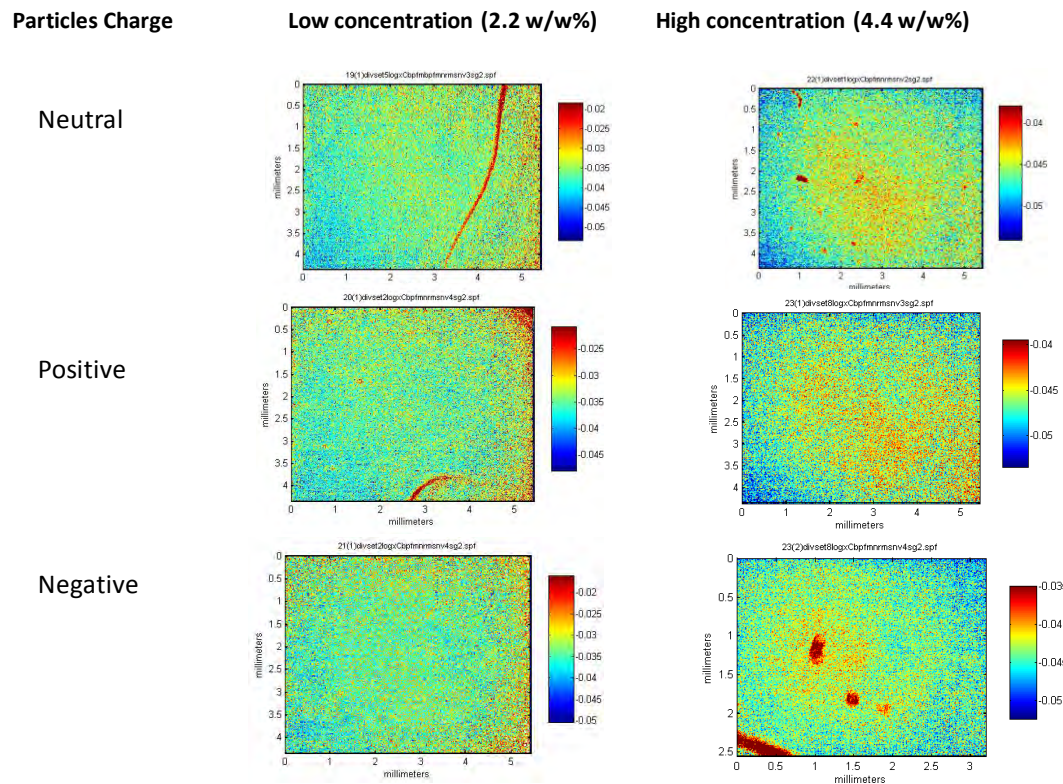


Figure III.2 Chemical imaging of negative membrane with 100 nm particles at high and low concentration at 2260 nm

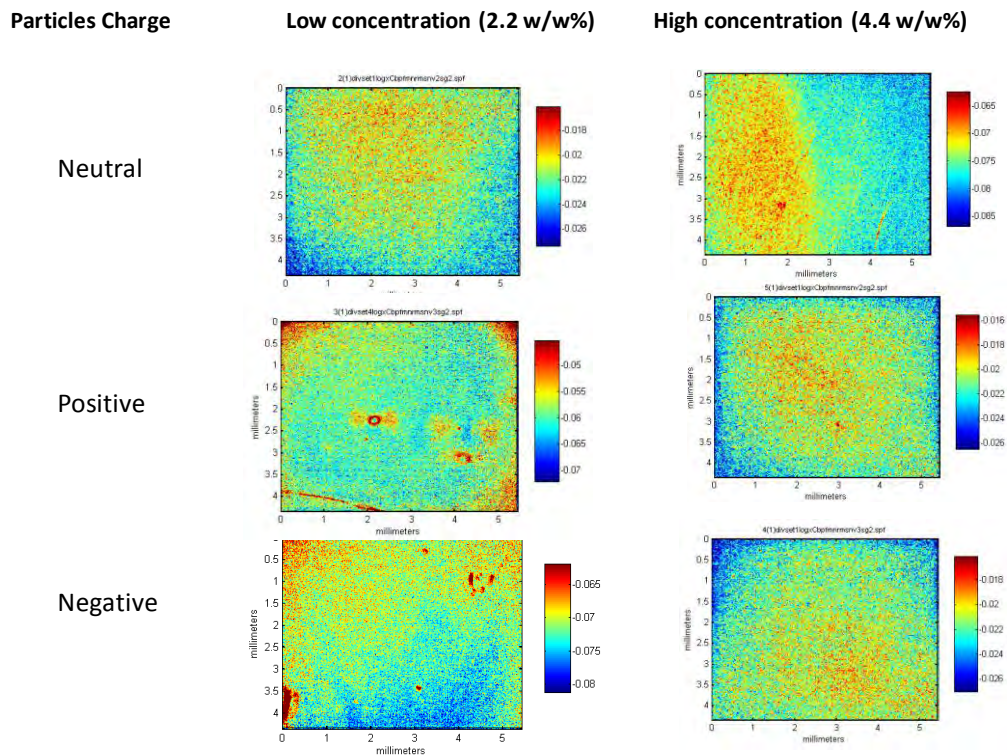


Figure III.3 Chemical imaging of neutral membrane with 100 nm particles at high and low concentration at 2260 nm